Supporting Information for:

Use of ^{15}N NMR Spectroscopy to Probe Covalency in a Thorium Nitride

Selena L. Staun,[†] Dumitru-Claudiu Sergentu,[‡] Guang Wu,[†] Jochen Autschbach,*[‡] and Trevor W. Hayton*[†]

[†]Department of Chemistry and Biochemistry, University of California, Santa Barbara, California 93106, United States

[‡]Department of Chemistry, 312 Natural Sciences Complex, University at Buffalo, State University of New York, Buffalo, NY 14260-3000, USA

*To whom correspondence should be addressed.

Email: hayton@chem.ucsb.edu, jochena@buffalo.edu

Table of Contents

Experimental Details	S3
NMR Spectra	S15
X-ray Crystallographic Data	S28
IR Spectra	S30
Computational Details	S39
References	S56

Experimental Details

General. All reactions and subsequent manipulations were performed under anaerobic and anhydrous conditions under an atmosphere of nitrogen. Hexanes, Et_2O, toluene were dried using a Vacuum Atmospheres DRI-SOLV Solvent Purification system and stored over 3Å sieves for 24 h prior to use. THF was dried by distillation from sodium/ benzophenone, and stored over 3Å sieves for 24 h prior to use. Benzene-d_6 and THF-d_8 were dried over 3Å molecular sieves for 24 h prior to use. $[Th(\mathit{C}H_2SiMe_2\mathit{N}SiMe_3)(NR_2)_2]$[1] (R = $SiMe_3$) and $[K(DME)][Th\{\mathit{N}(R)(SiMe_2\mathit{C}H_2)\}_2(NR_2)]$[2] were synthesized according to the previously reported procedures. All other reagents were purchased from commercial suppliers and used as received.

NMR spectra were recorded on an Agilent Technologies 400-MR DD2 400 MHz Spectrometer. ^1H NMR spectra were referenced to external tetramethylsilane (TMS) using the residual protio solvent peaks as internal standards. $^{13}C\{^1H\}$ NMR spectra were referenced indirectly with the ^1H resonance of TMS at 0.0 ppm, according to IUPAC standard,[3, 4] using the residual solvent peaks as internal standards. ^{15}N NMR spectra were referenced to CH_3NO_2 (δ = 0.0 ppm) as external standard. IR spectra were recorded on a Nicolet 6700 FT-IR spectrometer with a NXR FT Raman Module. Elemental analyses were performed by the Micro-Analytical Facility at the University of California, Berkeley.

X-ray Crystallography. Data for **[Na][1]**, **[K][1]**, and **2** were collected on a Bruker KAPPA APEX II diffractometer equipped with an APEX II CCD detector using a TRIUMPH monochromator with a Mo Kα X-ray source (α = 0.71073 Å). The crystals were mounted on a cryoloop under Paratone-N oil, and all data were collected at 100(2) K using an Oxford nitrogen gas cryostream. Data were collected using ω scans with 0.5° frame widths. Frame exposures of 15, 10, and 5 seconds were used for **[Na][1]**, **[K][1]**, and **2**, respectively. Data collection and cell parameter determinations were conducted using the SMART program.[5] Integration of the data frames and final cell parameter refinements were performed using SAINT software.[6] Absorption corrections of the data were carried out using the multi-scan method SADABS.[7] Subsequent calculations were carried out using SHELXTL.[8] Structure determination was done using direct or Patterson methods and difference Fourier techniques. All hydrogen atom positions were idealized, and rode on the atom of attachment. Structure solution, refinement, graphics, and creation of publication materials were performed using SHELXTL.[8]

Crystals of complex **[Na][1]** were only weakly diffracting. As a result, the six $N(SiMe_3)_2$ groups were constrained using SADI and EADP to all have the same temperature factors and geometries. For **[K][1]**, the six $N(SiMe_3)_2$ groups were found to be disordered over two positions in a 50:50 ratio. As a result, the six $N(SiMe_3)_2$ groups were constrained using SADI and EADP to all have the same temperature factors and geometries. In additon, the THF fragment ligated to the K^+ cation was also disordered over two positions in a 50:50 ratio. Its carbon atoms were also constrained using SADI and EADP. The crystal of complex **2** was found to be disordered over two positions in a 50:50 ratio. As a result, the six $N(SiMe_3)_2$ groups were constrained using SADI and EADP to have the same geometries. Becasue of the extensive disorder, hydrogen atoms were only assigned to one of the disordered carbon atoms.

Computational details. The structures were fully optimized with density functional theory (DFT) using the Amsterdam Density Functional (ADF) package, version 2017.[9] The B3LYP[10-12] hybrid exchange-correlation functional was employed in conjunction with all-electron triple-ζ doubly polarized (TZ2P) basis sets for all atoms. Scalar-relativistic (SR) effects were treated with the all-electron zero-order regular approximation (ZORA) relativistic Hamiltonian.[13] An atom-pairwise correction for dispersion forces was included via Grimme's D3 model augmented with the Becke-Johnson (BJ) damping.[14, 15]

Nuclear shielding calculations were performed with ADF, at the DFT/ ZORA-SR and DFT/spin-orbit (SO) ZORA levels. The PBE0[16, 17] and B3LYP hybrid exchange-correlation functionals were used, together with TZ2P basis sets for Th and N, and double-ζ polarized (DZP) basis sets for H, C and Si. Solvent effects were treated with the conductor-like screening model (COSMO).[18, 19] The ZORA-SO shielding calculations included the DFT exchange-correlation response.[20] The calculated nuclear shieldings (σ_{calc}, ppm) were converted to chemical shifts (δ_{calc}, ppm) relative to shielding of nitromethane (in nitromethane solvent) or ammonia (in ammonia solvent), calculated at the same level. To avoid issues with the NMR self-consistent field (SCF) step for the Th-nitride complex, no explicit 'AddDiffuseFit' or "Dependency" settings were used.

The equilibrium geometries obtained with ADF were subjected to Gaussian 16 (G16)[21] single-point DFT/B3LYP calculations, that used the def2-TZVP[9] basis set for N, the def2-SVP[22] basis sets for H, C and Si, and the small-core ECP60MDF pseudopotential with the associated [14s13p10d8f6g]/[6s6p5d4f3g] valence pseudo-orbital basis set for Th.[23] The results were used for natural localized molecular orbital (NLMO) analyses, performed with the NBO6 package.[24] Vibrational frequency calculations were conducted, with G16, on top of fully re-optimized geometries using the aforementioned computational details.

Synthesis of [Na(18-crown-6)(Et_2O)][(R_2N)$_3$Th(μ-N)(Th(NR_2)$_3$] (R = $SiMe_3$) ([Na][1]). To a stirring, cold (-25 °C), pale yellow solution of [Th{*N*(R)($SiMe_2$)*C*H_2}(NR_2)$_2$] (204.1

mg, 0.287 mmol) in THF (3 mL) was added $NaNH_2$ (11.3 mg, 0.290 mmol). No obvious change was observed upon addition. To this mixture was added a cold (-25 °C) solution of 18-crown-6 (75.5 mg, 0.286 mmol) in THF (2 mL). The reaction mixture was allowed to warm to room temperature with stirring. After 24 h, the volatiles were removed *in vacuo* from the cloudy, pale yellow suspension to provide an off-white solid. The solid was then extracted into diethyl ether (6 mL) and the resulting pale-yellow, cloudy suspension was filtered through a Celite column supported on glass wool (0.5 × 2 cm). The filtrate was concentrated *in vacuo* to 2 mL, layered with pentane (4 mL), and stored at -25 °C for 24 h, which resulted in the deposition of colorless crystalline solid. The solid was isolated by decanting the supernatant and then dried *in vacuo* to yield **[Na][1]** (106.6 mg). The supernatant was dried *in vacuo*, and the resulting off white solid was dissolved in diethyl ether (4 mL) and filtered through a Celite column supported on glass wool (0.5 × 2 cm). The filtrate was concentrated *in vacuo* to 2 mL, layered with pentane (6 mL), and stored at -25 °C for 24 h, which resulted in the deposition of more colorless crystalline solid (62.7 mg). Total yield: 169.3 mg, 66% yield. Anal. Calcd for $C_{48}H_{132}NaN_7O_6Si_{12}Th_2 \cdot C_4H_{10}O$: C, 34.66; H, 7.94; N, 5.44. Anal. Calcd for $C_{48}H_{132}NaN_7O_6Si_{12}Th_2$: C, 33.37; H, 7.70; N, 5.68. Found: C, 33.17; H, 7.77; N, 5.81. ^1H NMR (400 MHz, 25 °C, THF-d_8): δ 0.36 (s, 108H, NSiCH_3), 3.62 (s, 24H, 18-crown-6). $^{13}C\{^1H\}$ NMR (100 MHz, 25 °C, THF-d_8): δ 8.21 (s, NSiCH_3), 71.80 (s, 18-crown-6). IR (KBr pellet, cm^{-1}): 411 (s), 415 (m, sh), 422 (s), 430 (s), 438 (s), 451 (m, sh), 457 (s), 465 (s), 480 (w), 494 (m), 505 (m), 538 (s), 569 (s), 596 (s), 604 (s, sh), 656 (m, sh), 661 (s), 681 (s, sh), 692 (m, sh), 733 (m, sh), 742 (s, asym ν_{ThNTh}), 756 (s), 773 (s), 820 (m, sh), 829 (m), 843 (m, sh), 860 (s), 885 (m, sh), 939 (s), 962 (s, sh), 991 (s), 1020 (m, sh), 1041 (s), 1059 (s), 1076 (m, sh), 1107 (s), 1136 (m, sh), 1155 (m, sh), 1176 (m, sh), 1219 (m, sh), 1240 (m, sh), 1248 (s), 1250 (s), 1298 (s), 1335 (s), 1354 (s), 1367 (m, sh), 1385 (s), 1412 (m), 1433 (m, sh), 1446 (m, sh), 1456 (s), 1466 (s), 1495 (s), 1930 (w), 1969 (s), 1973 (s), 2089 (s), 2337 (w), 2360 (m), 2704 (m, sh), 2723 (m, sh), 2740 (s), 2812 (m, sh), 2858 (m, sh), 2875 (m, sh), 2899 (s), 2914 (m, sh), 2949 (s), 3377 (w).

Synthesis of [K(18-crown-6)(THF)$_2$][(R$_2$N)$_3$Th(μ-N)(Th(NR$_2$)$_3$] ([K][1]). To a stirring, cold (-25 °C), pale yellow solution of [K(DME)][Th{*N*(R)(SiMe$_2$*C*H$_2$)}$_2$(NR$_2$)] (315.8 mg, 0.376 mmol) in THF (5 mL) was added finely ground NH_4Cl (10.3 mg, 0.193 mmol). The reaction mixture was allowed to warm to room temperature with stirring. After 2 h, a solution of 18-crown-6 (49.7 mg, 0.188 mmol) in THF (2 mL) was added to the reaction mixture. After stirring for a further 30 min, the volatiles were removed *in vacuo* from the cloudy, pale yellow suspension to provide an off-white solid. The solid was then extracted into diethyl ether (6 mL) and the resulting pale-yellow, cloudy suspension was filtered through a Celite column supported on glass wool (0.5 × 2 cm). The filtrate was dried *in vacuo* to yield an off white powder, which was rinsed with toluene (3 × 4 mL) to separate **[K][1]** from unreacted [K(DME)][Th{*N*(R)(SiMe$_2$*C*H$_2$)}$_2$(NR$_2$)]. The soluble [K(DME)][Th{*N*(R)(SiMe$_2$*C*H$_2$)}$_2$(NR$_2$)] was decanted away from the solid and discarded. The remaining white microcrystalline powder was dried *in vacuo*, dissolved in a mixture of diethyl ether (4 mL) and THF (2 mL), and filtered through a Celite column supported on glass wool (0.5 × 2 cm). The colorless filtrate was concentrated *in vacuo* to 2 mL, layered with pentane (4 mL), and stored at -25 °C for 24 h, which resulted in the deposition of colorless crystalline solid. The solid was isolated by decanting the supernatant and dried *in vacuo* to yield **[K][1]** (15 mg, 5% yield). Anal. Calcd for $C_{48}H_{132}KN_7O_6Si_{12}Th_2\cdot 2C_4H_8O$:

C, 35.63; H, 7.90; N, 5.19. Anal. Calcd for $C_{48}H_{132}KN_7O_6Si_{12}Th_2$: C, 33.06; H, 7.63; N, 5.62. Found: C, 33.13; H, 7.54; N, 5.32. ^{1}H NMR (400 MHz, 25 °C, THF-d_8): δ 0.36 (s, 108H, NSiC*H*$_3$), 3.63 (s, 24H, 18-crown-6). ^{13}C{^{1}H} NMR (100 MHz, 25 °C, THF-d_8): δ 8.22 (s, NSi*C*H$_3$), 72.03 (s, 18-crown-6). IR (KBr pellet, cm^{-1}): 409 (s), 420 (s), 472 (w), 499 (w), 526 (s), 596 (s), 604 (s), 615 (w, sh), 656 (s), 669 (w, sh), 677 (m, sh), 694 (w, sh), 742 (s, asym ν_{ThNTh}), 752 (m, sh), 773 (s), 802 (m, sh), 820 (m, sh), 831 (w), 839 (m, sh), 864 (s), 937 (m), 962 (s), 1032 (w), 1059 (s), 1111 (s), 1132 (m, sh), 1180 (m), 1248 (s), 1252 (w, sh), 1267 (m, sh), 1282 (s), 1352 (s), 1365 (w, sh), 1396 (m), 1433 (m), 1454 (s), 1473 (s), 1848 (w), 1923 (m), 1977 (s), 2075 (m), 2141 (w), 2245 (w), 2364 (m), 2467 (m), 2598 (w), 2632 (w), 2686 (s), 2708 (s), 2744 (s), 2796 (s), 2827 (s), 2897 (s), 2947 (s).

Synthesis of [K(18-crown-6)(THF)$_2$][(R$_2$N)$_3$Th(μ-^{15}N)(Th(NR$_2$)$_3$] ([K][1-^{15}N]). To a stirring, cold (-25 °C), pale yellow solution of [K(DME)][Th{*N*(R)(SiMe$_2$*C*H$_2$)}$_2$(NR$_2$)] (300.7 mg, 0.358 mmol) in THF (3 mL) was added finely ground ^{15}NH$_4$Cl (9.7 mg, 0.273 mmol). The reaction mixture was allowed to warm to room temperature with stirring. After 2 h, a solution of 18-crown-6 (48.3 mg, 0.183 mmol) in THF (2 mL) was added to the reaction mixture. After stirring for 1 h further, the volatiles were removed *in vacuo* from the cloudy, pale yellow suspension to provide an off-white solid. The solid was then extracted into diethyl ether (6 mL) and the resulting pale-yellow, cloudy suspension was filtered through a Celite column supported on glass wool (0.5 × 2 cm). The filtrate was dried *in vacuo* to yield an off white powder, which was rinsed with toluene (3 × 4 mL) to separate **[K][1-^{15}N]** from unreacted [K(DME)][Th{*N*(R)(SiMe$_2$*C*H$_2$)}$_2$(NR$_2$)]. The soluble [K(DME)][Th{*N*(R)(SiMe$_2$*C*H$_2$)}$_2$(NR$_2$)] was decanted away from the solid and discarded.

The remaining white microcrystalline powder was dried *in vacuo*, dissolved in a mixture of diethyl ether (4 mL) and THF (2 mL), and filtered through a Celite column supported on glass wool (0.5 × 2 cm). The filtrate was concentrated *in vacuo* to 2 mL, layered with pentane (4 mL), and stored at -25 °C for 24 h, which resulted in the deposition of colorless crystalline solid. The solid was isolated by decanting the supernatant and then dried *in vacuo* to yield **[K][1-^{15}N]** (43.2 mg, 13% yield). ^{1}H NMR (400 MHz, 25 °C, THF-d_8): δ 0.36 (s, 108H, NSiCH_3), 3.63 (s, 24H, 18-crown-6). ^{15}N{^{1}H} NMR (40 MHz, 25 °C, THF-d_8): δ 298.79 (s, (μ-N)). IR (KBr pellet, cm^{-1}): 409 (s), 422 (s), 436 (s), 442 (m), 447 (m, sh), 469 (m), 476 (m), 488 (w), 492 (m, sh), 528 (s), 592 (s), 604 (s), 613 (w, sh), 652 (s), 658 (w), 669 (m), 677 (m, sh), 690 (m, sh), 735 (s, asym ν_{ThNTh}), 756 (s), 773 (s), 820 (m, sh), 831 (w), 843 (m), 864 (s), 904 (m, sh), 943 (s), 962 (s), 1028 (s), 1059 (s), 1113 (s), 1132 (m, sh), 1182 (s), 1248 (s), 1252 (m, sh), 1269 (m, sh), 1282 (s), 1352 (s), 1363 (m, sh), 1390 (m, sh), 1400 (s), 1433 (s), 1454 (s), 1473 (s), 1925 (m), 1975 (s), 2075 (w), 2135 (w), 2251 (w), 2347 (w), 2463 (w), 2586 (w), 2638 (w), 2688 (s), 2708 (s), 2744 (s), 2796 (m), 2825 (s), 2877 (m, sh), 2897 (s), 2947 (s), 2958 (m, sh), 3130 (m, sh).592 (s), 652 (s), 733 (m), 833 (m), 945 (m), 1059 (s), 1113 (s), 1182 (s), 1248 (m), 1352 (s), 1473 (s), 2897 (w).

Synthesis of [Th(NR$_2$)$_3$(NH$_2$)] (R = SiMe$_3$) (2). To a stirring, cold (-25 °C), pale yellow solution of [Th{*N*(R)(SiMe$_2$)*C*H$_2$}(NR$_2$)$_2$] (97.4 mg, 0.137 mmol) in THF (2 mL) was added a THF solution of NH$_3$ (1.0 mL, 0.4 mmol, 0.4 M). The pale yellow reaction mixture was allowed to warm to room temperature with stirring. After 1 h, the volatiles were removed *in vacuo* to provide an off-white solid. The solid was then extracted into pentane (3 mL) and the resulting pale-yellow, cloudy suspension was filtered through a Celite column supported on glass wool (0.5 × 2 cm). The filtrate was transferred to a 4 mL vial, which was placed inside a 20 mL scintillation vial and iso-octane (2 mL) was added to the outer vial. Storage of this two-vial system at -25 °C for 7 d resulted in the deposition of a colorless crystalline solid. The solid was isolated by decanting the supernatant and then dried *in vacuo* to yield **2** (13.2 mg). The supernatant was transferred to a new 4 mL vial, which was placed inside a 20 mL scintillation vial and iso-octane (2 mL) was added to the outer vial. Storage of this two-vial system at -25 °C for 7 d resulted in the deposition of more colorless crystalline solid (37.9 mg). Total yield: 51.1 mg, 51% yield. Anal. Calcd for $C_{18}H_{56}N_4Si_6Th$: C, 29.65; H, 7.74; N, 7.68. Found: C, 29.78; H, 7.87; N, 7.49. ^{1}H NMR (400 MHz, 25 °C, C_6D_6): δ 0.37 (s, 54H, NSiC*H*$_3$), 3.67 (t, 2H, N*H*$_2$, J_{NH} = 45.8 Hz). $^{13}C\{^1H\}$ NMR (100 MHz, 25 °C, C_6D_6): δ 3.79 (s, *C*H$_3$). IR (KBr pellet, cm^{-1}): 415 (m, sh), 424 (s), 430 (m, sh), 455 (w), 496 (s), 607 (s), 660 (s), 671 (m, sh), 735 (m, sh), 756 (m, sh), 769 (s), 822 (m, sh), 841 (m, sh), 860 (m), 957 (s), 1038 (m, sh), 1115 (m, sh), 1126 (s), 1182 (s), 1246 (s), 1259 (m, sh), 1284 (m, sh), 1344 (m), 1358 (m, sh), 1400 (s), 1421 (m), 1439 (m), 1493 (m, sh), 1508 (s), 1560 (s), 1610 (s), 1857 (s), 1919 (s), 1994 (m), 2013 (w), 2083 (m), 2233 (w), 2347 (m), 2478 (s), 2582 (m), 2638 (m), 2791 (m, sh), 2819 (s), 2897 (s), 2926 (s), 2949 (s), 3140 (m), 3201 (m, sh), 3321 (s, ν_{NH}).

Synthesis of $[Th(NR_2)_3(^{15}NH_2)]$ (2-^{15}N). A pale yellow solution of $[Th\{N(R)(SiMe_2)CH_2\}(NR_2)_2]$ (215.7 mg, 0.303 mmol) in THF (13 mL) was added to a 20 mL Schlenk tube fitted with a rotaflow valve. The Schlenk tube was removed from the glovebox, attached to a vacuum line, the headspace was evacuated, and gaseous $^{15}NH_3$ (1 atm, 7 mL, 0.291 mmol) was added to the Schlenk flask. The Schlenk tube was allowed to stand for 30 min, brought back into the glovebox, and the pale yellow reaction mixture was transferred to a 20 mL vial. The volatiles were removed *in vacuo* to provide a pale yellow oily solid. The solid was extracted into pentane (3 mL) and the resulting pale-yellow, cloudy suspension was filtered through a Celite column supported on glass wool (0.5 × 2 cm). The filtrate was transferred to a 4 mL vial, which was placed inside a 20 mL scintillation vial and iso-octane (2 mL) was added to the outer vial. Storage of this two-vial system at -25 °C for 7 d resulted in the deposition of colorless crystalline solid. The solid was isolated by decanting the supernatant and then dried *in vacuo* to yield **2-^{15}N** (188.8 mg, 85% yield). ^{1}H NMR (400 MHz, 25 °C, C_6D_6): δ 0.36 (s, 54H, NSiC*H*$_3$), 3.67 (d, 2H, N*H*$_2$, J_{NH} = 62.3 Hz). ^{1}H{^{15}N} (400 MHz, 25 °C, C_6D_6): δ 0.36 (s, 54H, NSiC*H*$_3$), 3.67 (N*H*$_2$). ^{15}N{^{1}H} NMR (40 MHz, 25 °C, C_6D_6): δ -198.4 (s, *N*H$_2$). IR (KBr pellet, cm^{-1}): 407 (m, sh), 413 (s), 422 (s), 432 (m, sh), 445 (w), 482 (s, ν_{ThN}), 486 (s), 513 (m, sh), 565 (m, sh), 607 (s), 660 (s), 675 (w, sh), 735 (m, sh), 756 (m, sh), 773 (s), 812 (m, sh), 864 (w), 906 (w), 955 (w), 1014 (m, sh), 1045 (m, sh), 1115 (s), 1126 (s), 1182 (m), 1244 (s), 1259 (m, sh), 1284 (m, sh), 1340 (m, sh), 1358 (m, sh), 1400 (s), 1425 (s), 1439 (m, sh), 1468 (m, sh), 1504 (s), 1626 (m), 1632 (m, sh), 1662 (s), 1859 (s), 1919 (s), 1986 (w), 2040 (s), 2081 (m), 2231 (w), 2330 (m), 2359 (s), 2476 (s), 2640 (m), 2791 (m, sh), 2819 (s), 2897 (s), 2947 (s), 3140 (m), 3211 (w), 3317 (s, ν_{NH}), 3377 (w).

NMR scale reaction of [Th{*N*(R)(SiMe$_2$)*C*H$_2$}(NR$_2$)$_2$] with NaNH$_2$. An NMR tube fitted with a J-Young valve was charged with [Th{*N*(R)(SiMe$_2$)*C*H$_2$}(NR$_2$)$_2$] (23.4 mg, 0.0329 mmol), NaNH$_2$ (1.6 mg, 0.0410 mmol), and THF-*d*$_8$ (0.5 mL). To this pale yellow solution was added a colorless solution of 18-crown-6 (8.7 mg, 0.0329 mmol) in THF-*d*$_8$ (0.5 mL). A ^{1}H NMR spectrum was then recorded (Figure S12). ^{1}H NMR (400 MHz, 25 °C, THF-*d*$_8$): δ 0.11 (s, 9H, NSi(C*H*$_3$)$_3$), 0.22 (s, 6H, Si(C*H*$_3$)$_2$), 0.29 (s, 36H, N(Si(C*H*$_3$)$_3$)$_2$), 0.47 (s, 2H, $\mathrm{C}H_2$), 3.57 (s, 24H, 18-crown-6). The NMR tube was then attached to a wrist action tube shaker. After 150 min of shaking, a ^{1}H NMR spectrum was re-recorded. This spectrum revealed the appearance of a resonances corresponding to **[Na][1]** and **2**, concomitant with a decrease in the intensity of the resonances assignable to $[\mathrm{Th}\{N(\mathrm{R})(\mathrm{SiMe_2})C\mathrm{H_2}\}(\mathrm{NR_2})_2]$. ^{1}H NMR (400 MHz, 25 °C, THF-d_8): δ 0.11 (s, 9H, $\mathrm{NSi}(\mathrm{C}H_3)_3$), 0.22 (s, 6H, $\mathrm{Si}(\mathrm{C}H_3)_2$), 0.29 (s, 36H, $\mathrm{N}(\mathrm{Si}(\mathrm{C}H_3)_3)_2$), 0.30 (s, 54H, $\mathrm{NSiC}H_3$, **2**), 0.36 (s, 108H, $\mathrm{NSiC}H_3$, **[Na][1]**), 0.47 (s, 2H, $\mathrm{C}H_2$), 3.58 (s, 24H, 18-crown-6)). The NMR tube was then re-attached to a wrist action tube shaker. After 7 h and 30 min of shaking, a ^{1}H NMR spectrum was re-recorded. This spectrum revealed the appearance of resonances assignable to $[\mathrm{Na}(\mathrm{THF}\text{-}d_8)_x][\mathrm{Th}\{N(\mathrm{R})(\mathrm{SiMe_2}C\mathrm{H_2})\}_2(\mathrm{NR_2})]$, while resonances assignable to **[Na][1]** and **2** grow in intensity, and peaks assignable to $[\mathrm{Th}\{N(\mathrm{R})(\mathrm{SiMe_2})C\mathrm{H_2}\}(\mathrm{NR_2})_2]$ continue to decrease in intensity. ^{1}H NMR (400 MHz, 25 °C, THF-d_8): δ -0.36 (br s, 4H, $\mathrm{C}H_2$, bis(metallacycle)), 0.03 (s, 12H, $\mathrm{N}(\mathrm{SiC}H_3)_2$, bis(metallacycle)), 0.04 (s, $\mathrm{NSi}(\mathrm{C}H_3)_3$, bis(metallacycle) overlapping with $\mathrm{HN}(\mathrm{SiMe_3})_2$), 0.11 (s, 9H, $\mathrm{NSi}(\mathrm{C}H_3)_3$), 0.18 (s, 18H, $\mathrm{N}(\mathrm{SiC}H_3)_2$, bis(metallacycle)), 0.22 (s, 6H, $\mathrm{Si}(\mathrm{C}H_3)_2$), 0.29 (s, 36H, $\mathrm{N}(\mathrm{Si}(\mathrm{C}H_3)_3)_2$), 0.30 (s, 54H, $\mathrm{NSiC}H_3$, **2**), 0.36 (s, 108H, $\mathrm{NSiC}H_3$, **[Na][1]**), 0.47 (s, 2H, $\mathrm{C}H_2$), 3.58 (s, 24H, 18-crown-6). The NMR tube was then re-attached to a wrist action tube shaker. After 32 h of shaking, the resonance assignable to **[Na][1]** is the most prominent peak in the spectrum, the resonances assignable to **2** and $[\mathrm{Th}\{N(\mathrm{R})(\mathrm{SiMe_2})C\mathrm{H_2}\}(\mathrm{NR_2})_2]$ have disappeared, and only a small amount of $[\mathrm{Na}(\mathrm{THF}\text{-}d_8)_x][\mathrm{Th}\{N(\mathrm{R})(\mathrm{SiMe_2}C\mathrm{H_2})\}_2(\mathrm{NR_2})]$ remains in the sample. ^{1}H NMR (400 MHz, 25 °C, THF-d_8): δ -0.36 (br s, 4H, $\mathrm{C}H_2$, bis(metallacycle)), 0.03 (s, 12H, $\mathrm{N}(\mathrm{SiC}H_3)_2$, bis(metallacycle)), 0.04 (s, $\mathrm{NSi}(\mathrm{C}H_3)_3$, bis(metallacycle) overlapping with $HN(SiMe_3)_2$), 0.18 (s, 18H, $N(SiC\mathit{H}_3)_2$, bis(metallacycle)), 0.36 (s, 108H, $NSiC\mathit{H}_3$, **[Na][1]**), 3.60 (s, 24H, 18-crown-6).

NMR scale reaction of $[K(DME)][Th\{\mathit{N}(R)(SiMe_2\mathit{C}H_2)\}_2(NR_2)]$ with $[Th(NR_2)_3(NH_2)]$ (2). A colorless solution of $[K(DME)][Th\{\mathit{N}(R)(SiMe_2\mathit{C}H_2)\}_2(NR_2)]$ (4.7 mg, 0.0056 mmol) in THF-d_8 (0.5 mL) was added to an NMR tube fitted with a J-Young valve. A ^1H NMR spectrum was recorded (Figure S13). ^1H NMR (400 MHz, 25 °C, THF-d_8): δ -0.36 (br s, 4H, $C\mathit{H}_2$), 0.02 (s, 12H, $N(SiC\mathit{H}_3)_2$), 0.04 (s, 18H, $NSi(C\mathit{H}_3)_3$), 0.18 (s, 18H, $N(Si(C\mathit{H}_3)_3)_2$), 3.27 (s, 6H, $OC\mathit{H}_3$), 3.42 (s, 4H, $OC\mathit{H}_2$). The NMR tube was brought back into the glovebox, and a colorless solution of **2** (4.1 mg, 0.0056 mmol) in THF-d_8 (0.5 mL) was added to the tube. After 15 min, a ^1H NMR spectrum was taken, which revealed the presences of resonances assignable to both **2** and bis(metallacycle). ^1H NMR (400 MHz, 25 °C, THF-d_8): δ -0.36 (br s, 4H, $C\mathit{H}_2$), 0.02 (s, 12H, $N(SiC\mathit{H}_3)_2$), 0.04 (s, 18H, $NSi(C\mathit{H}_3)_3$), 0.18 (s, 18H, $N(Si(C\mathit{H}_3)_3)_2$), 0.30 (s, 54H, $NSiC\mathit{H}_3$, **2**), 3.27 (s, 6H, $OC\mathit{H}_3$), 3.42 (s, 4H, $OC\mathit{H}_2$), 3.99 (t, 2H, $N\mathit{H}_2$, **2**). 18-crown-6 (2.1 mg, 0.0080 mmol) was then added to the reaction mixture as a crystalline solid. No obvious change was observed upon addition. A ^1H NMR spectrum was re-recorded after 4 h. This spectrum revealed the presence of small amounts of **[K][1]**, along with resonances assignable to both **2** and bis(metallacycle). ^1H NMR (400 MHz, 25 °C, THF-d_8): δ -0.36 (br s, 4H, $C\mathit{H}_2$), 0.02 (s, 12H, $N(SiC\mathit{H}_3)_2$), 0.04 (s, 18H, $NSi(C\mathit{H}_3)_3$), 0.18 (s, 18H, $N(Si(C\mathit{H}_3)_3)_2$), 0.30 (s, 54H, $NSiC\mathit{H}_3$, **2**), 0.36 (s, 108H, $NSiC\mathit{H}_3$, **[K][1]**), 3.27 (s, 6H, $OC\mathit{H}_3$), 3.42 (s, 4H, $OC\mathit{H}_2$), 3.99 (t, 2H, $N\mathit{H}_2$, **2**). A ^1H NMR spectrum was re-recorded after 3 d. This spectrum revealed considerable increase in the amount of **[K][1]** present in the sample, while resonances corresponding to **2** and bis(metallacycle) have decreased in intensity. The ratio of

[K][1]:**2**:[K(DME)][Th{*N*(R)(SiMe$_2$*C*H$_2$)}$_2$(NR$_2$)] after 3 d was 1:3:6.7. ^{1}H NMR (400 MHz, 25 °C, THF-*d*$_8$): δ -0.36 (br s, 4H, C*H*$_2$), 0.02 (s, 12H, N(SiC*H*$_3$)$_2$), 0.04 (s, 18H, NSi(C*H*$_3$)$_3$), 0.18 (s, 18H, N(Si(C*H*$_3$)$_3$)$_2$), 0.30 (s, 54H, NSiC*H*$_3$, **2**), 0.36 (s, 108H, NSiC*H*$_3$, **[K][1]**), 3.27 (s, 6H, OC*H*$_3$), 3.42 (s, 4H, OC*H*$_2$), 3.99 (t, 2H, N*H*$_2$, **2**).

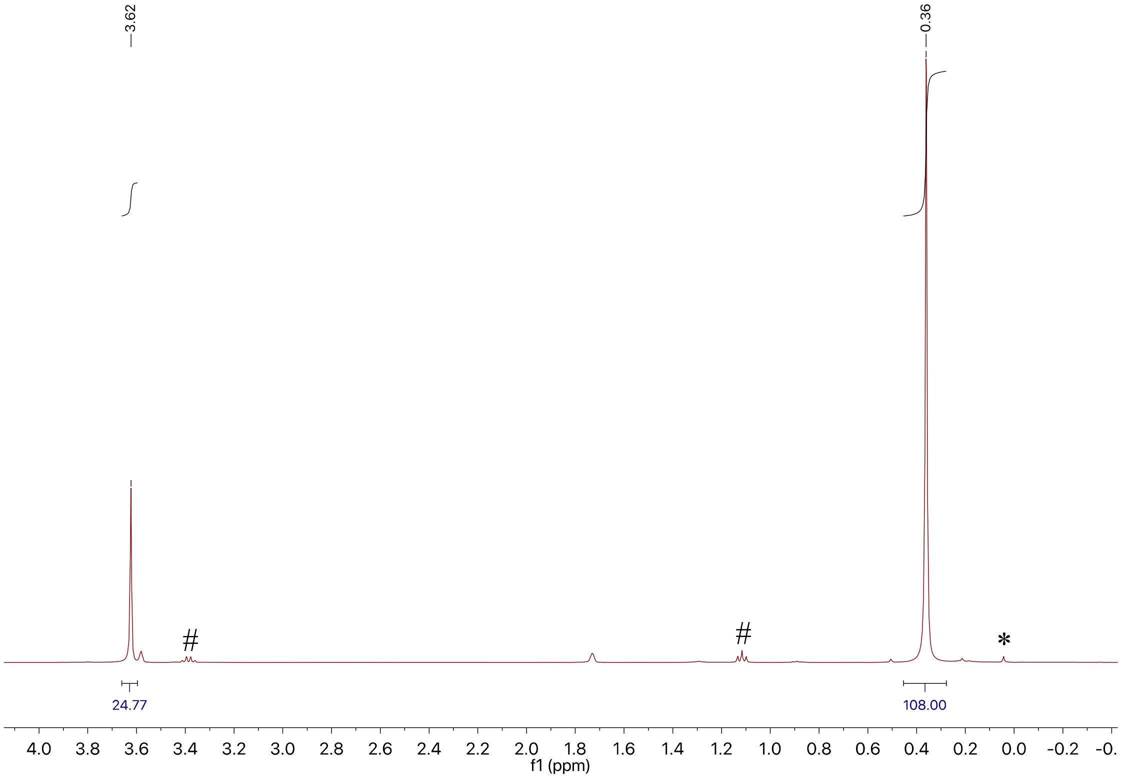

Figure S1. ^{1}H NMR spectrum of **[Na][1]** in THF-d_8. (*) indicates the presence of $HN(SiMe_3)_2$, (#) indicates the presence of Et_2O.

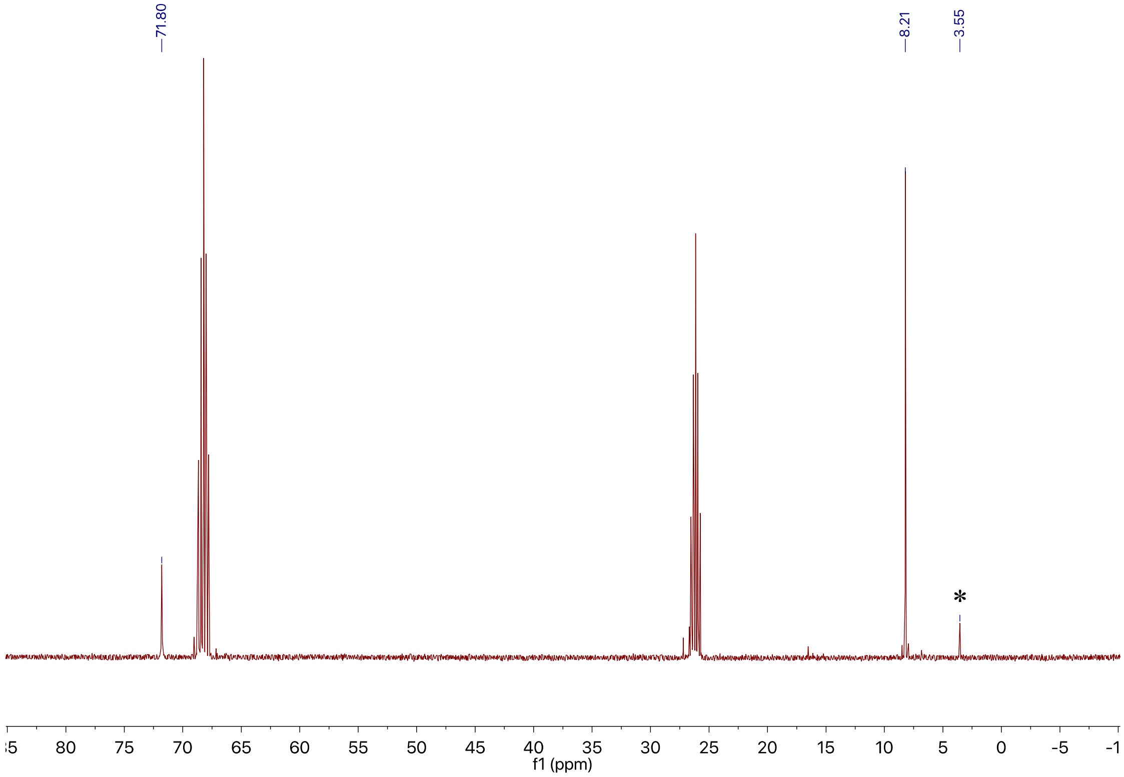

Figure S2. ^{13}C NMR spectrum of **[Na][1]** in THF-d_8. (*) indicates the presence of HN(SiMe$_3$)$_2$.

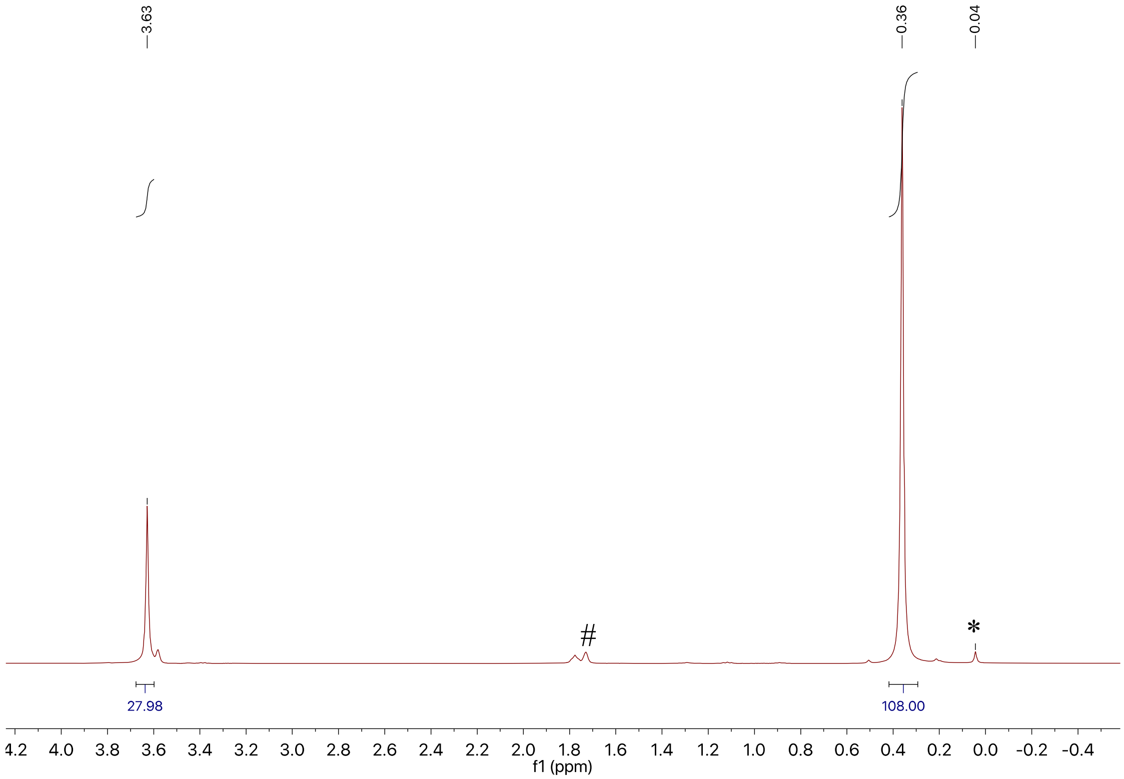

Figure S3. ^{1}H NMR spectrum of **[K][1]** in THF-d_8. (*) indicates the presence of HN(SiMe$_3$)$_2$. (#) indicates the presence of THF-h_8.

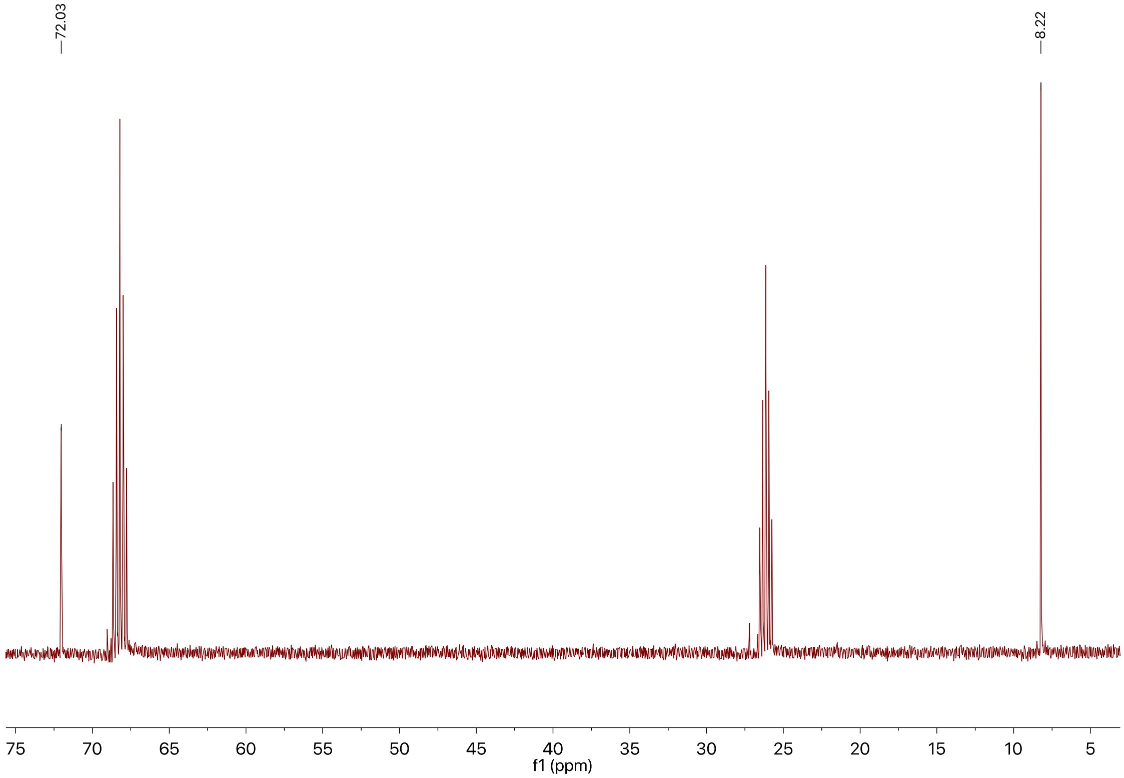

Figure S4. ^{13}C NMR spectrum of **[K][1]** in THF-d_8.

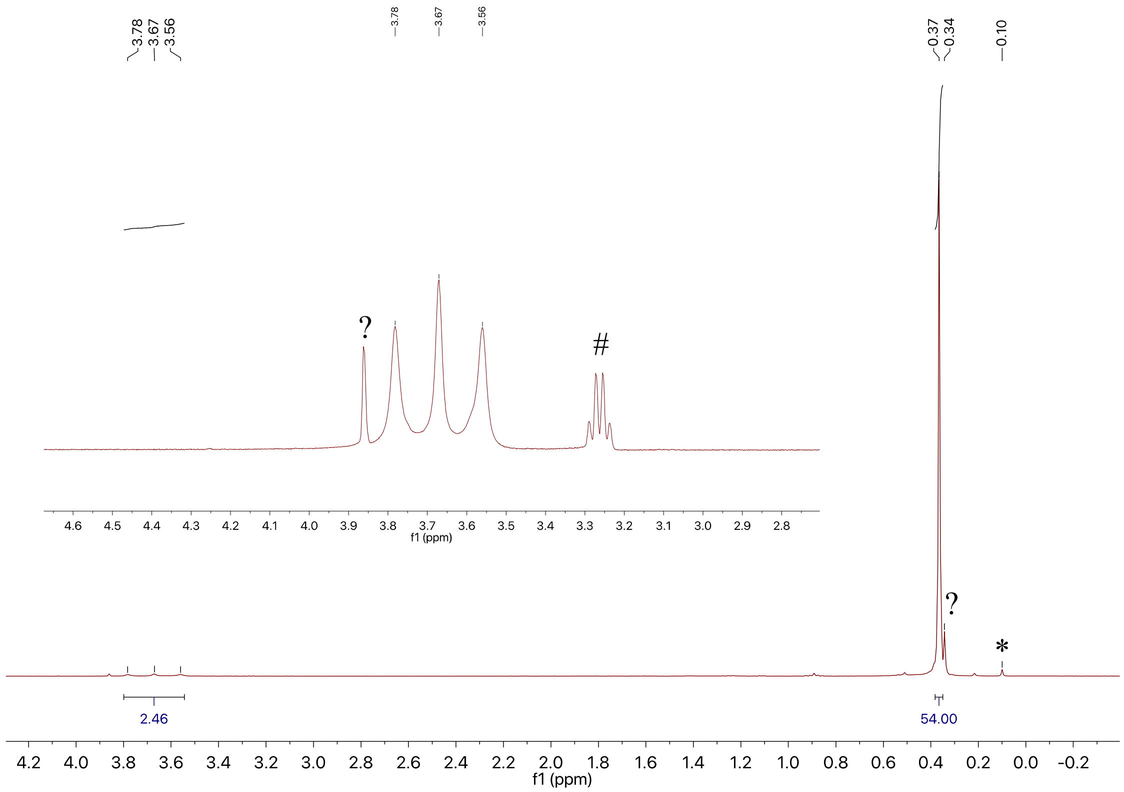

Figure S5. ^{1}H NMR spectrum of **2** in C_6D_6. The inset highlights the -NH_2 resonance. (*) indicates the presence of $HN(SiMe_3)_2$. (#) indicates the presence of Et_2O. (?) indicates the presence of unidentified products.

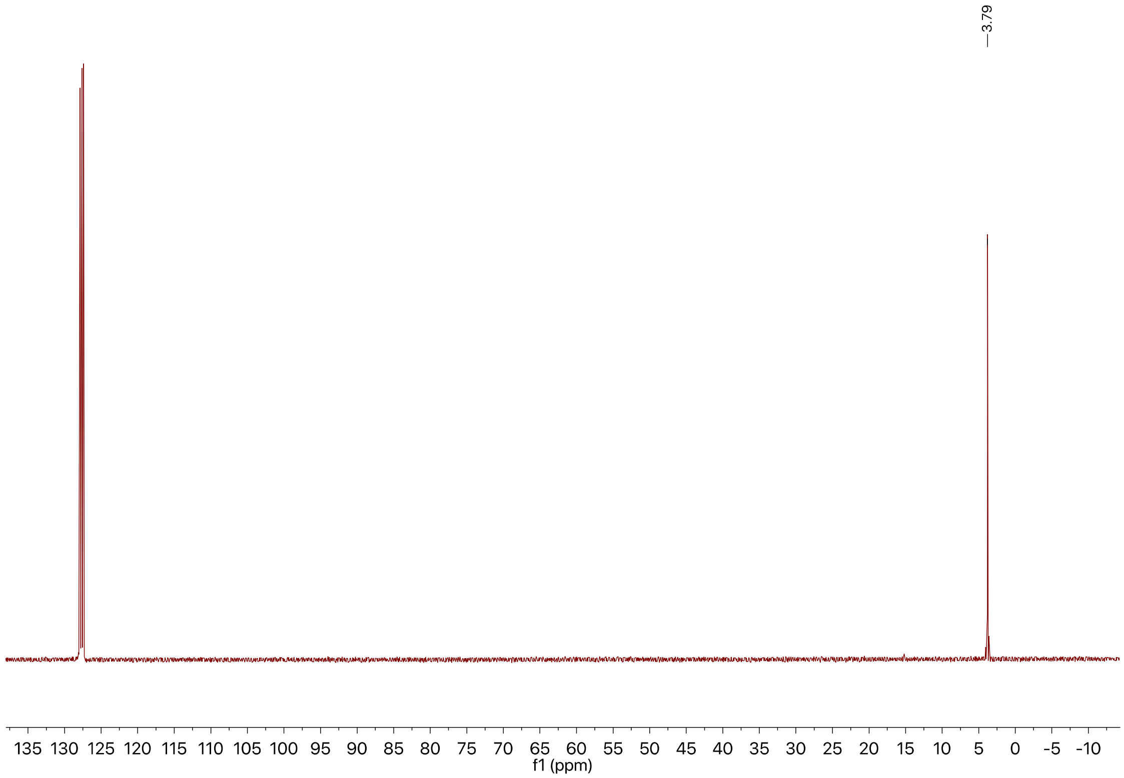

Figure S6. ^{13}C NMR spectrum of **2** in C_6D_6.

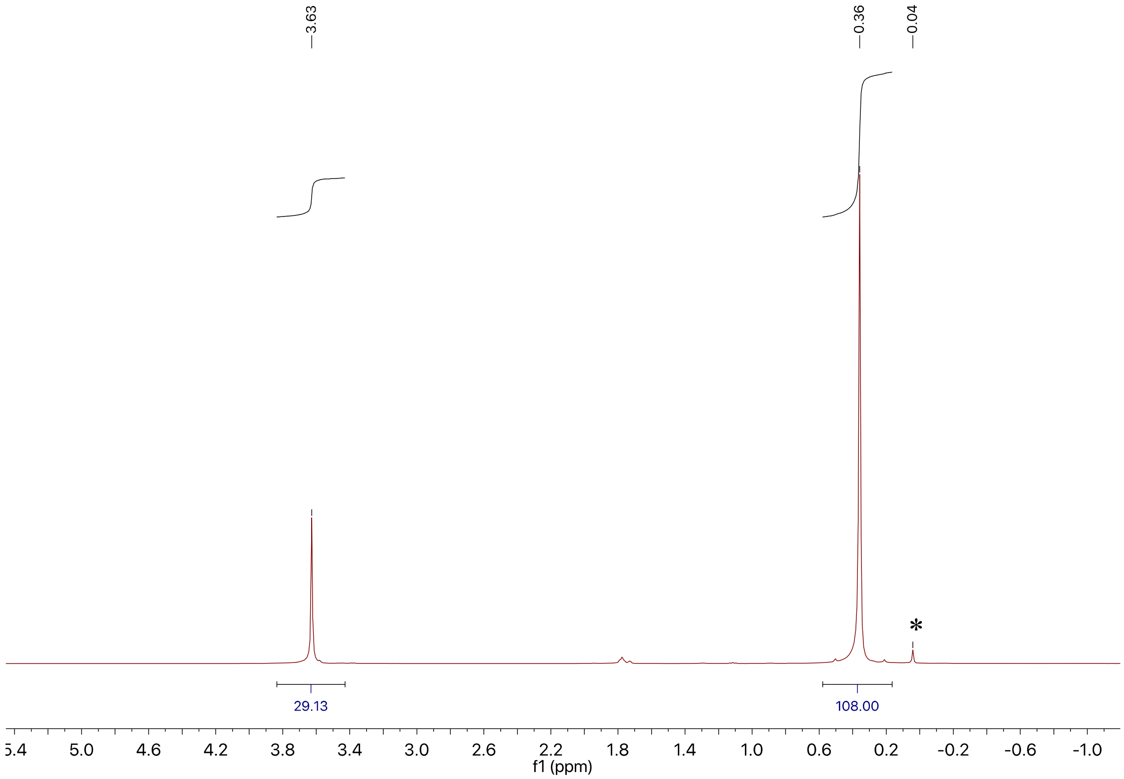

Figure S7. ^{1}H NMR spectrum of **[K][1-^{15}N]** in THF-d_8. (*) indicates the presence of HN(SiMe$_3$)$_2$.

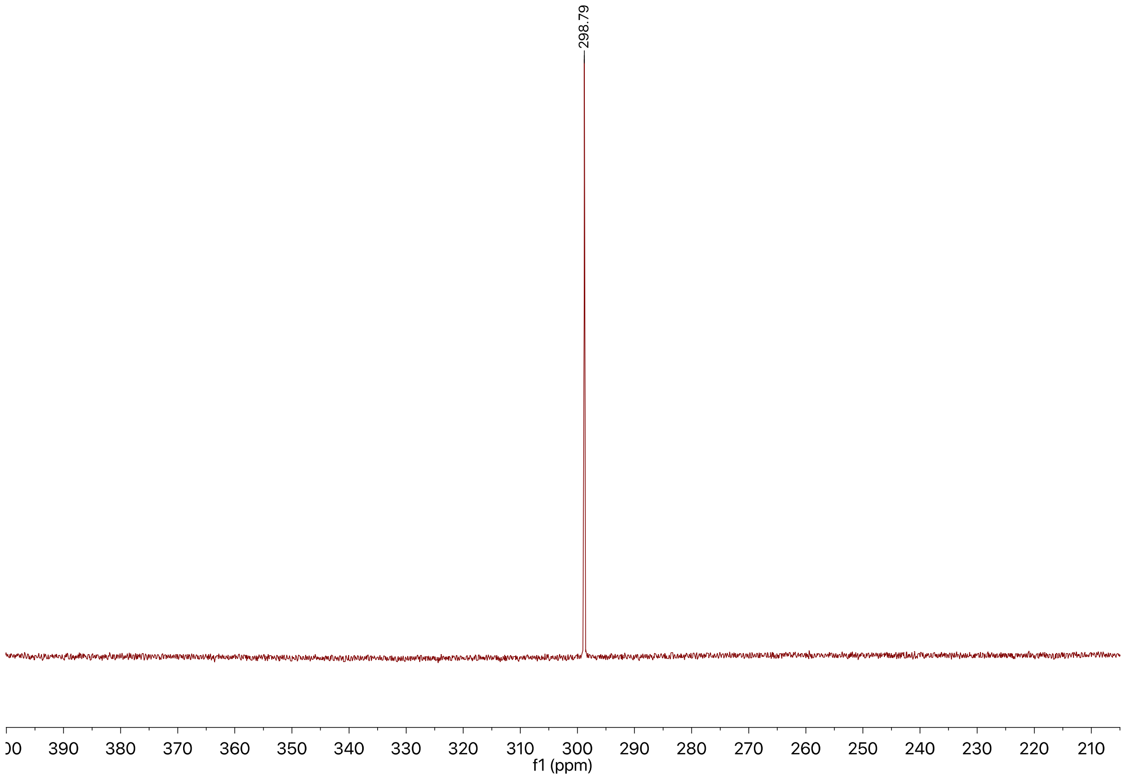

Figure S8. $^{15}N\{^{1}H\}$ NMR spectrum of **[K][1-^{15}N]** in THF-d_8.

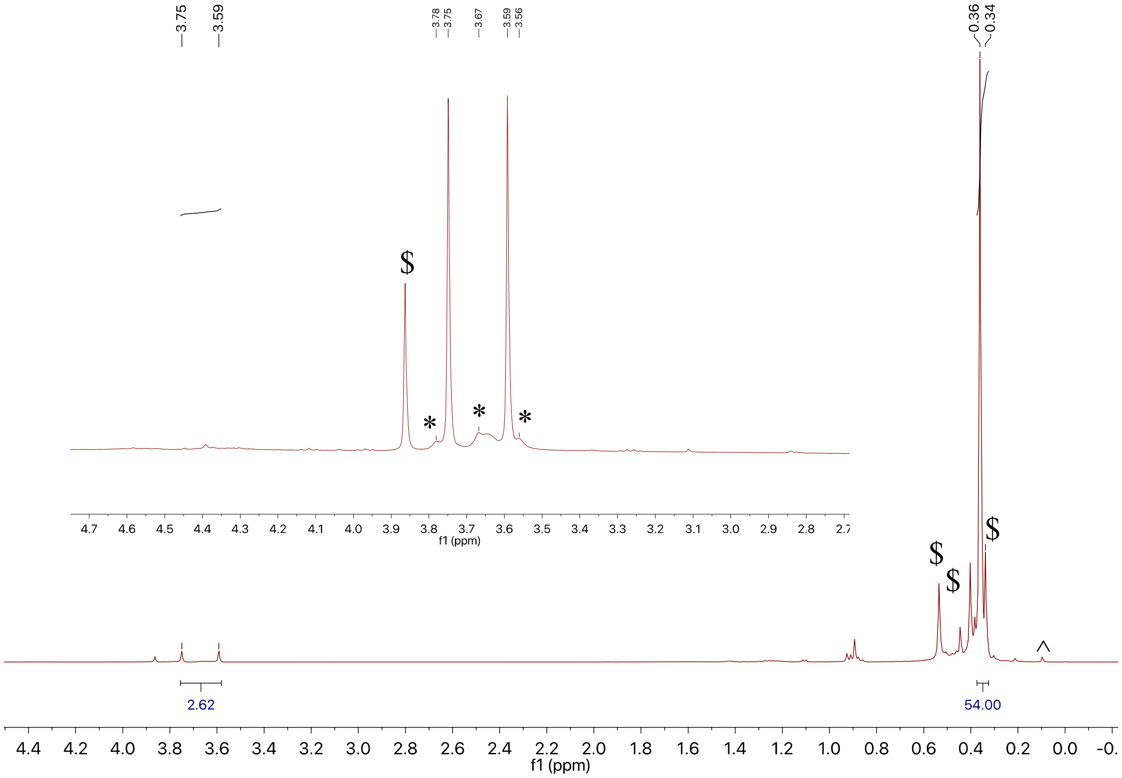

Figure S9. ^{1}H NMR spectrum of **2-^{15}N** in C_6D_6. The inset highlights the -NH_2 resonance. (*) indicated resonances assignable to a small amount of the ^{14}N isotopomer. ($) indicates the presence of unidentified products. (^) indicates the presence of $HN(SiMe_3)_2$.

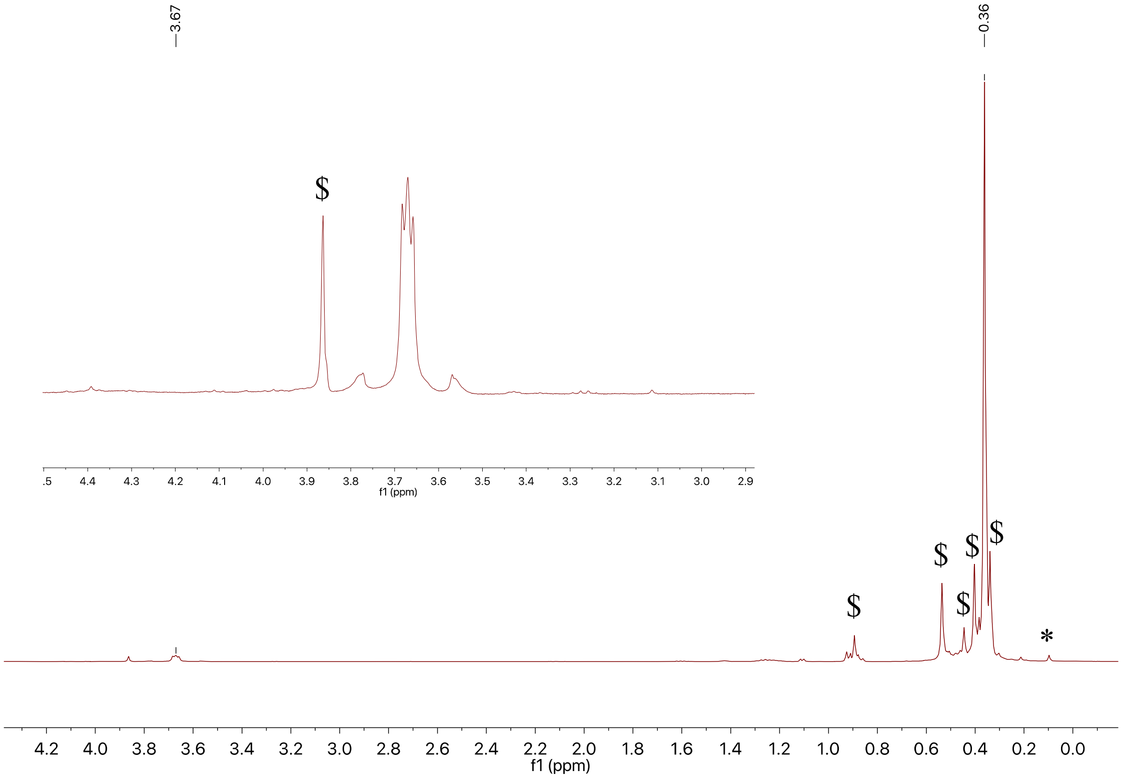

Figure S10. ${}^{1}H\{{}^{15}N\}$ NMR spectrum of **2-^{15}N** in C_6D_6. The inset highlights the $-NH_2$ resonance. ($) indicates the presence of unidentified products. (*) indicates the presence of $HN(SiMe_3)_2$.

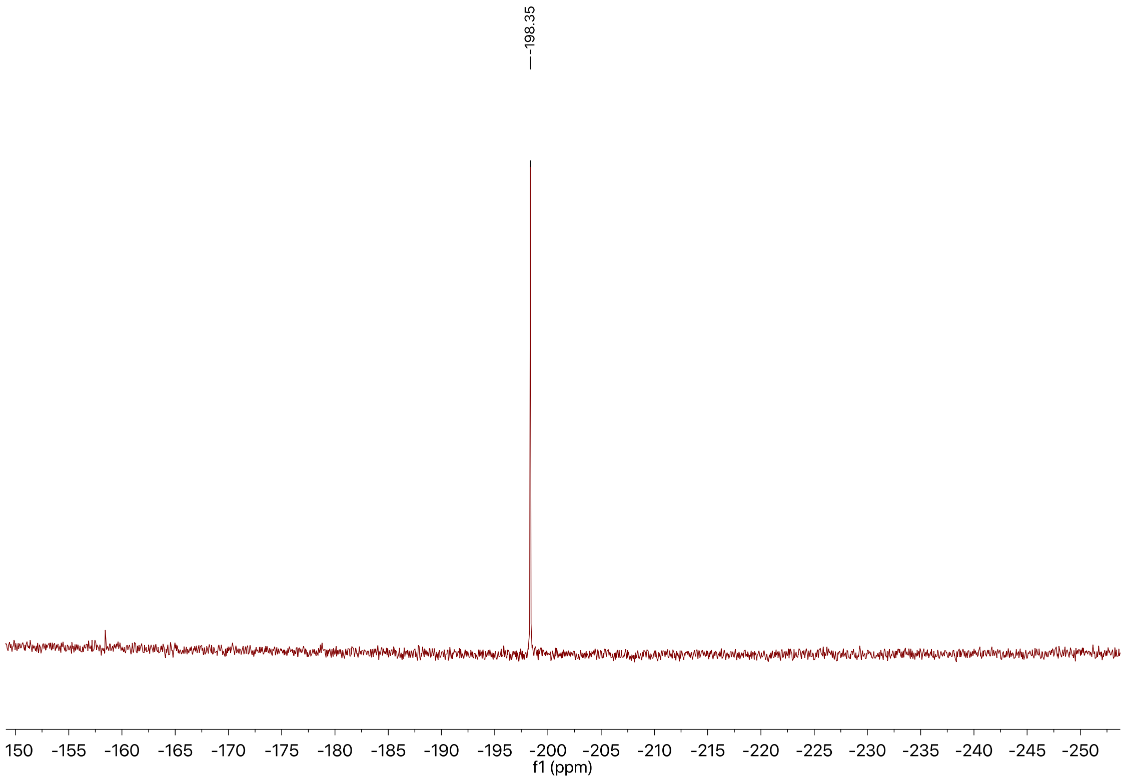

Figure S11. ^{15}N NMR spectrum of **2-^{15}N** in C_6D_6.

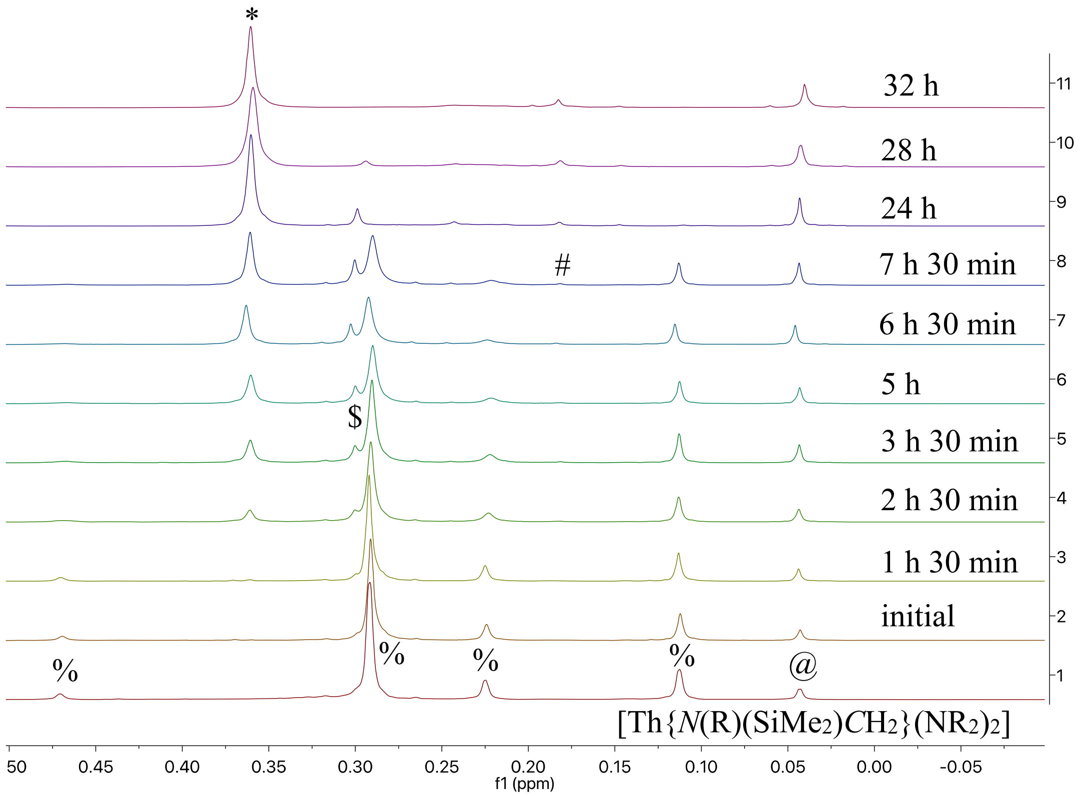

Figure S12. Partial *in situ* ^{1}H NMR spectrum of the reaction of [Th{*N*(R)(SiMe$_2$)*C*H$_2$}(NR$_2$)$_2$] (R = SiMe$_3$) with 1 equiv of NaNH$_2$ and 18-crown-6 in THF-*d*$_8$ over the course of 32 h. (*) indicates the presence of **[Na][1]**, (%) indicates the presence of [Th{*N*(R)(SiMe$_2$)*C*H$_2$}(NR$_2$)$_2$], (#) indicates the presence of [Na(THF-*d*$_8$)$_x$][Th{*N*(R)(SiMe$_2$*C*H$_2$)}$_2$(NR$_2$)], ($) indicates the presence of **2**, and (@) indicates the presence of HN(SiMe$_3$)$_2$.

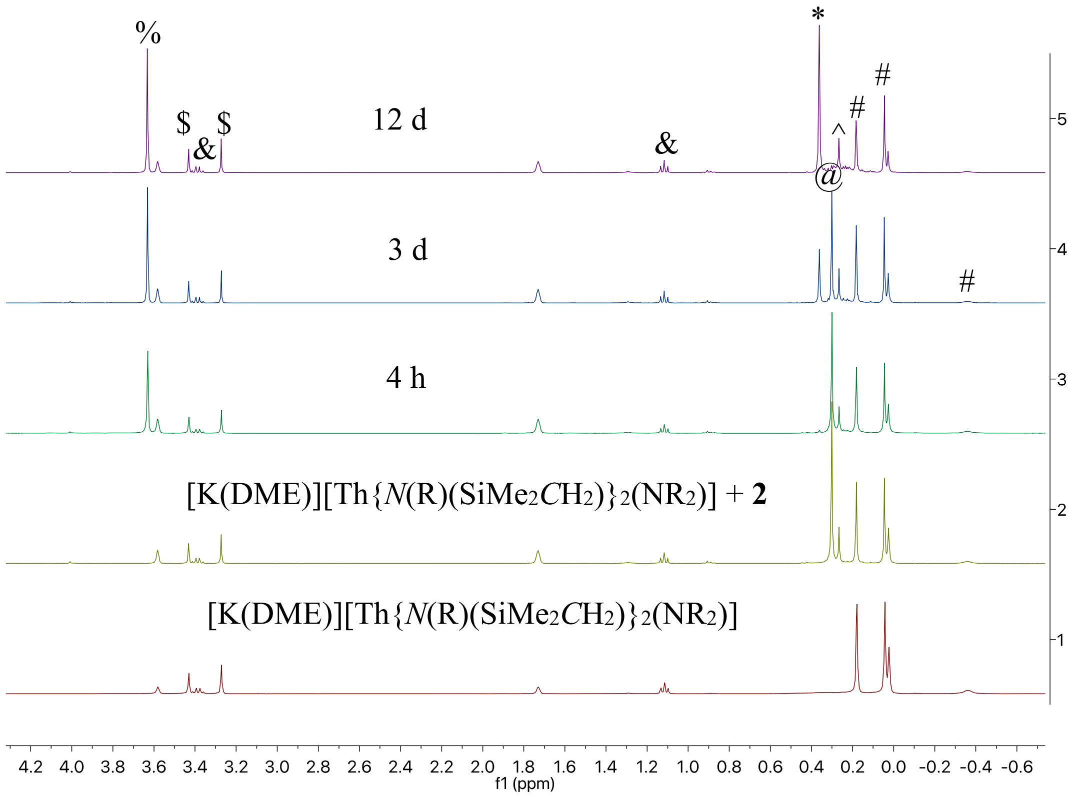

Figure S13. Partial *in situ* ^{1}H NMR spectrum of the reaction of [K(DME)][Th{*N*(R)(SiMe$_2$*C*H$_2$)}$_2$(NR$_2$)] (R = SiMe$_3$) with **2** and 18-crown-6 in THF-*d*$_8$ over 12 d. (*) indicates the presence of **[K][1]**, (@) indicates the presence of **2**, (#) indicates the presence of [K(DME)][Th{*N*(R)(SiMe$_2$*C*H$_2$)}$_2$(NR$_2$)], (%) indicates the presence of 18-crown-6, ($) indicates the presence of DME, (&) indicates the presence of Et$_2$O, and (^) indicates the presence of an unidentified product.

Table S1. X-ray Crystallographic Data for **[Na][1]**, **[K][1]**, and **2**.

	[Na][1]	**[K][1]**	**2**
empirical formula	$C_{52}H_{142}NaN_7O_7Si_{12}Th_2$	$C_{56}H_{148}KN_7O_8Si_{12}Th_2$	$C_{18}H_{56}N_4Si_6Th$
crystal habit, color	Block, Colorless	Block, Colorless	Block, Colorless
crystal size (mm)	0.2 × 0.1 × 0.05	0.15× 0.15 × 0.1	0.25 × 0.2 × 0.15
space group	*P*21/c	*P*-1	R-3c
volume (Å^3)	8593(16)	2238.6(10)	5029(3)
a (Å)	12.391(14)	11.893(3)	18.497(6)
b (Å)	23.18(2)	14.617(4)	18.497(6)
c (Å)	29.92(3)	14.620(4)	16.973(4)
α (deg)	90	74.546(15)	90
β (deg)	90.96(3)	71.051(15)	90
γ (deg)	90	71.238(14)	120
Z	4	1	6
formula weight (g/mol)	1801.87	1888.07	729.24
density (calculated) (Mg/m^3)	1.393	1.400	1.445
absorption coefficient (mm^{-1})	3.672	3.569	4.674
F_{000}	3672	964	2196
total no. reflections	31666	22425	8880
unique reflections	13515	9312	930
final R indices (I >2σ(I)]	R_1 = 0.1190 wR_2 = 0.1927	R_1 = 0.0804 wR_2 = 0.1803	R_1 = 0.0714 wR_2 = 0.1843
largest diff. peak and hole (e$^-$ A^{-3})	3.831 and -2.354	1.246 and -2.456	0.796 and -1.627
GOF	1.085	1.142	1.406

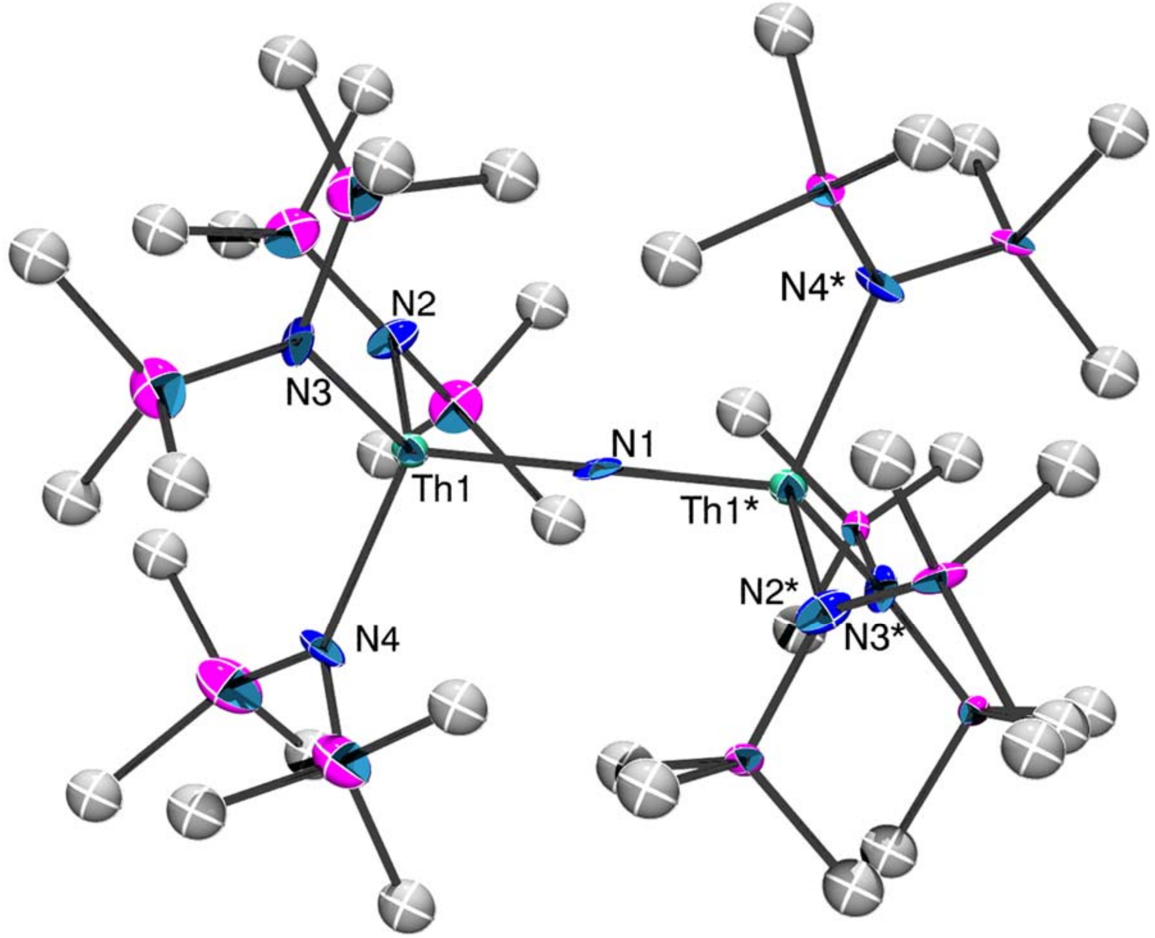

Figure S14. Solid-state molecular structure of **[K][1]**, with 50% probability ellipsoids. Hydrogen atoms and [K(18-crown-6)(THF)$_2$]$^+$ counterion removed for clarity. Selected bond lengths (Å) and angles (°): Th1-N1 = 2.1167(7), av. Th1–N$_{amido}$ = 2.41, Th1-N1-Th1* = 180, av. N$_{amido}$-Th1-N$_{amido}$ = 109.2.

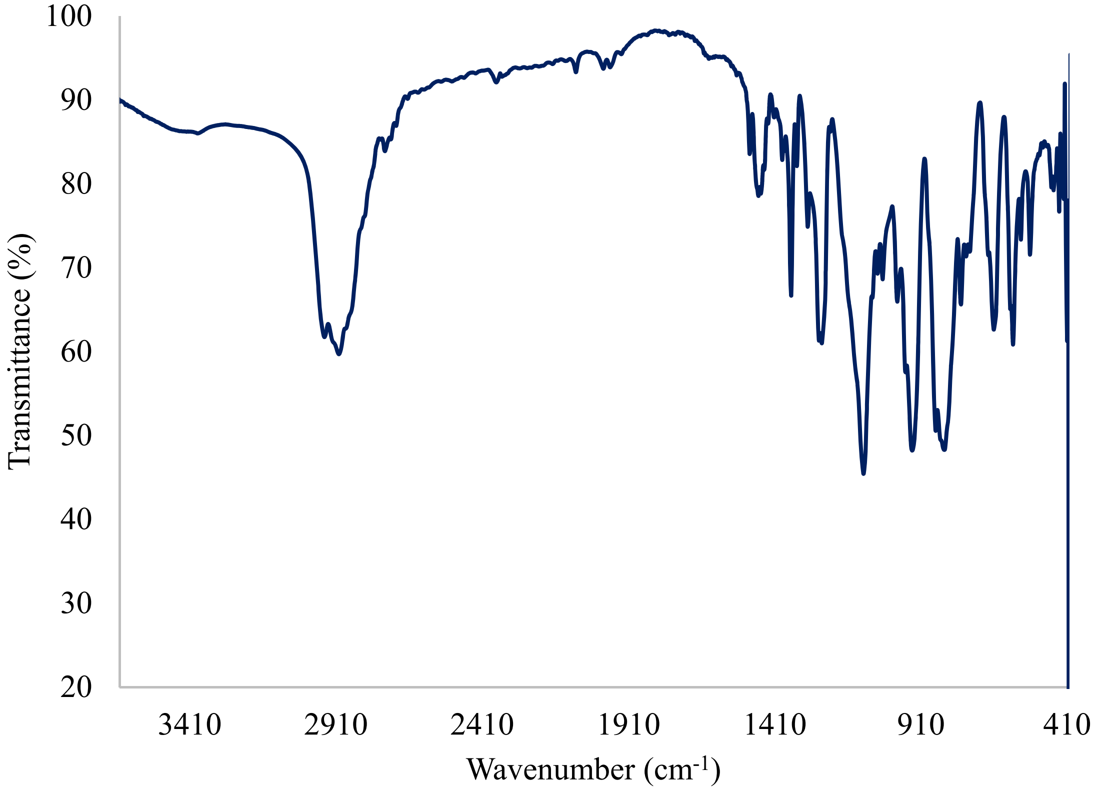

Figure S15. IR spectrum of **[Na][1]** (KBr pellet).

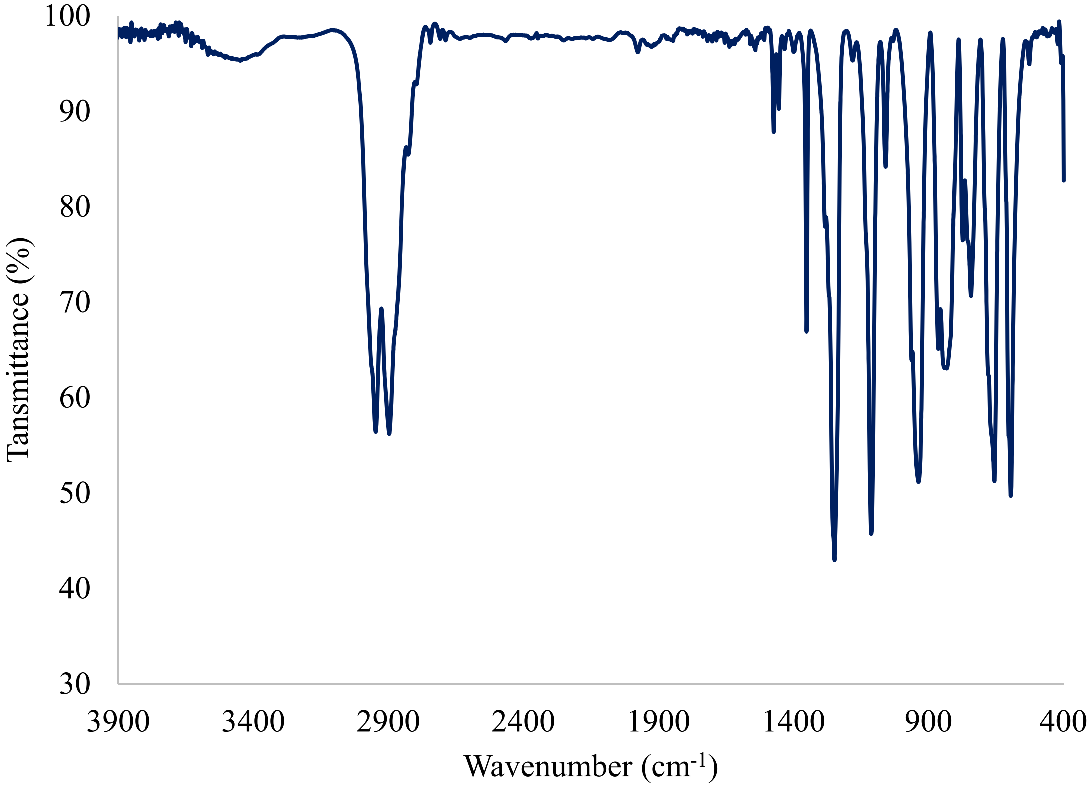

Figure S16. IR spectrum of **[K][1]** (KBr pellet).

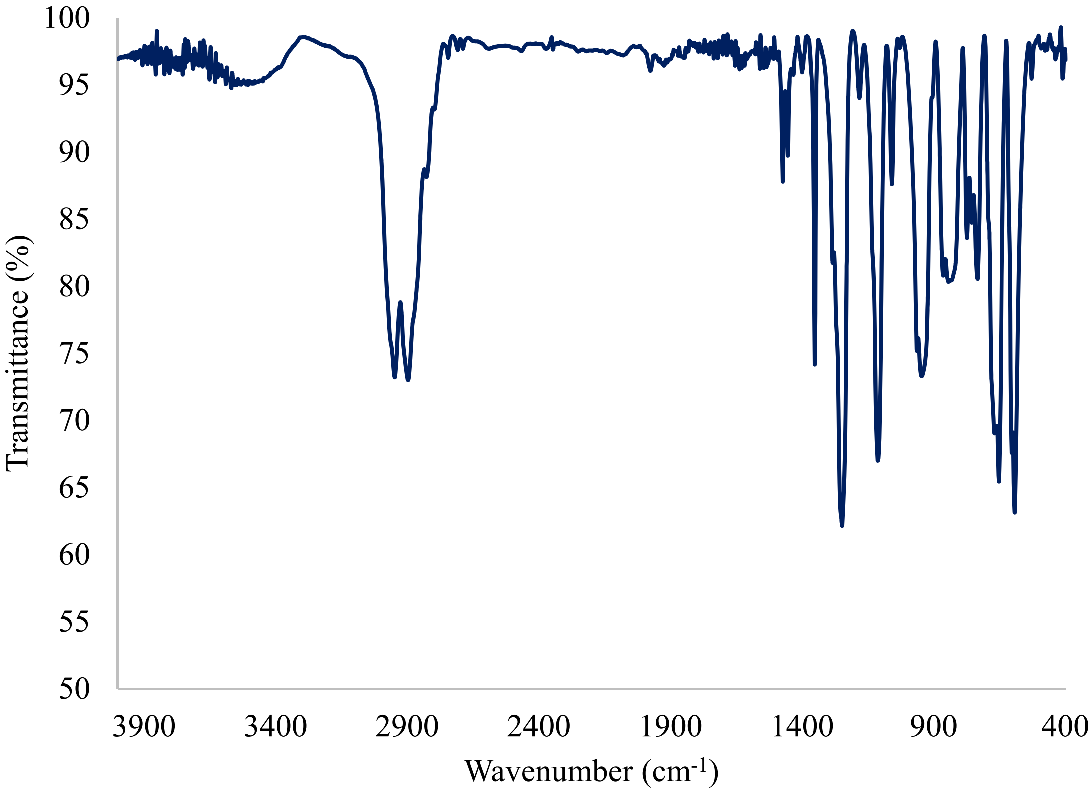

Figure S17. IR spectrum of **[K][1-^{15}N]** (KBr pellet).

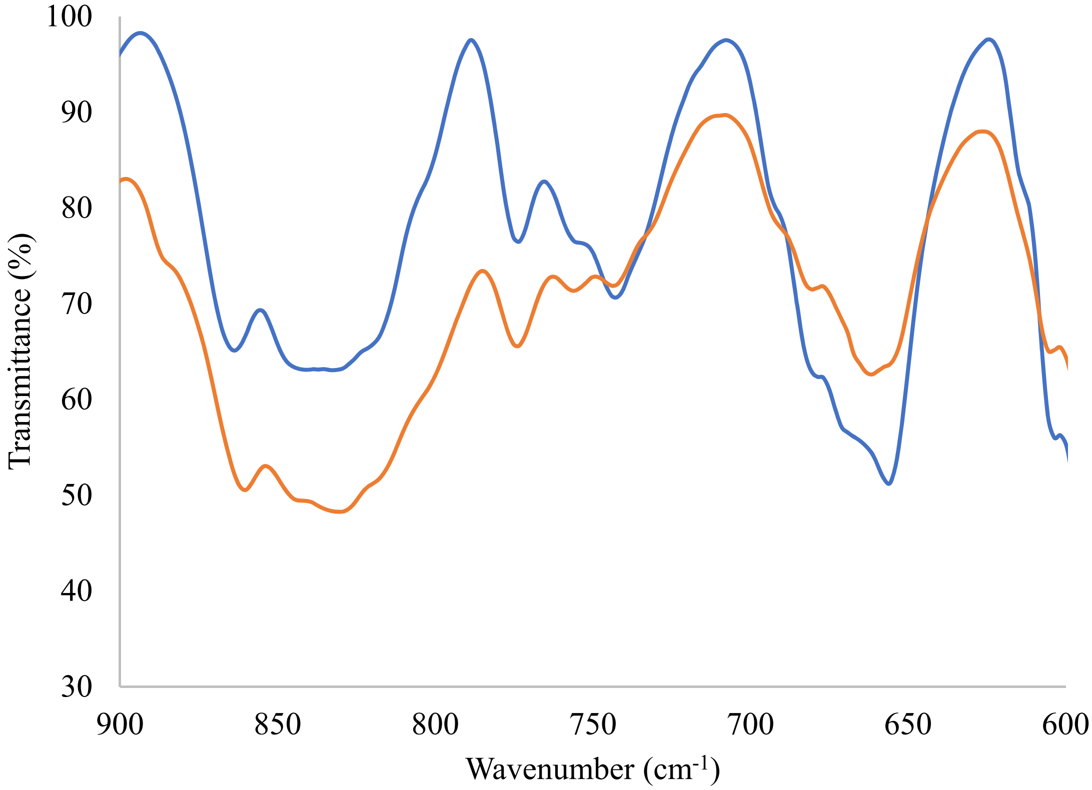

Figure S18. Partial IR spectrum of **[Na][1]** (orange) and **[K][1]** (blue) (KBr pellet).

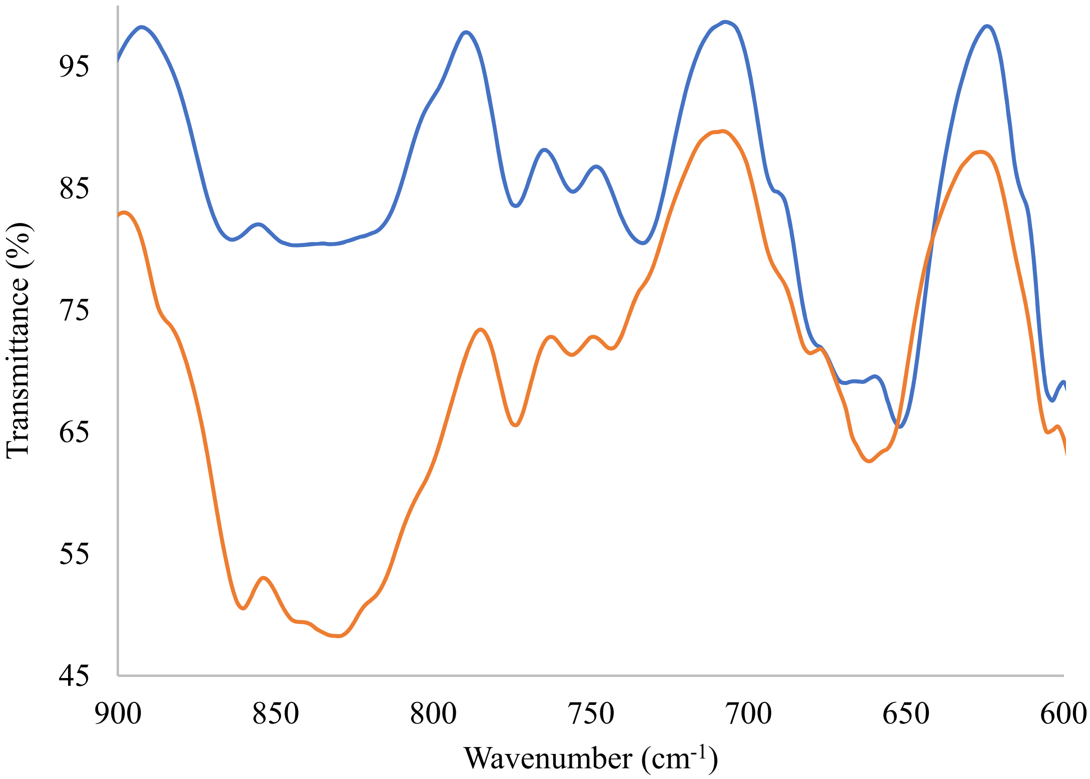

Figure S19. Partial IR spectra of **[Na][1]** (orange) and **[K][1-^{15}N]** (blue) (KBr pellet).

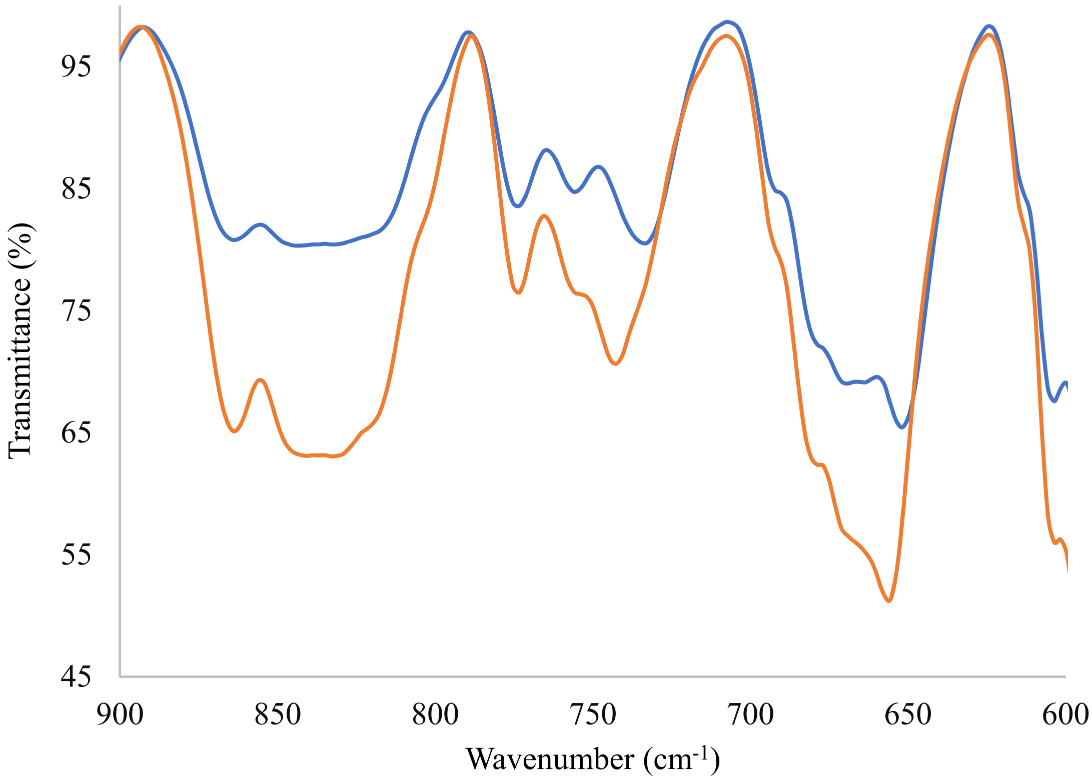

Figure S20. Partial IR spectra of **[K][1]** (orange) and **[K][1-^{15}N]** (blue) (KBr pellet).

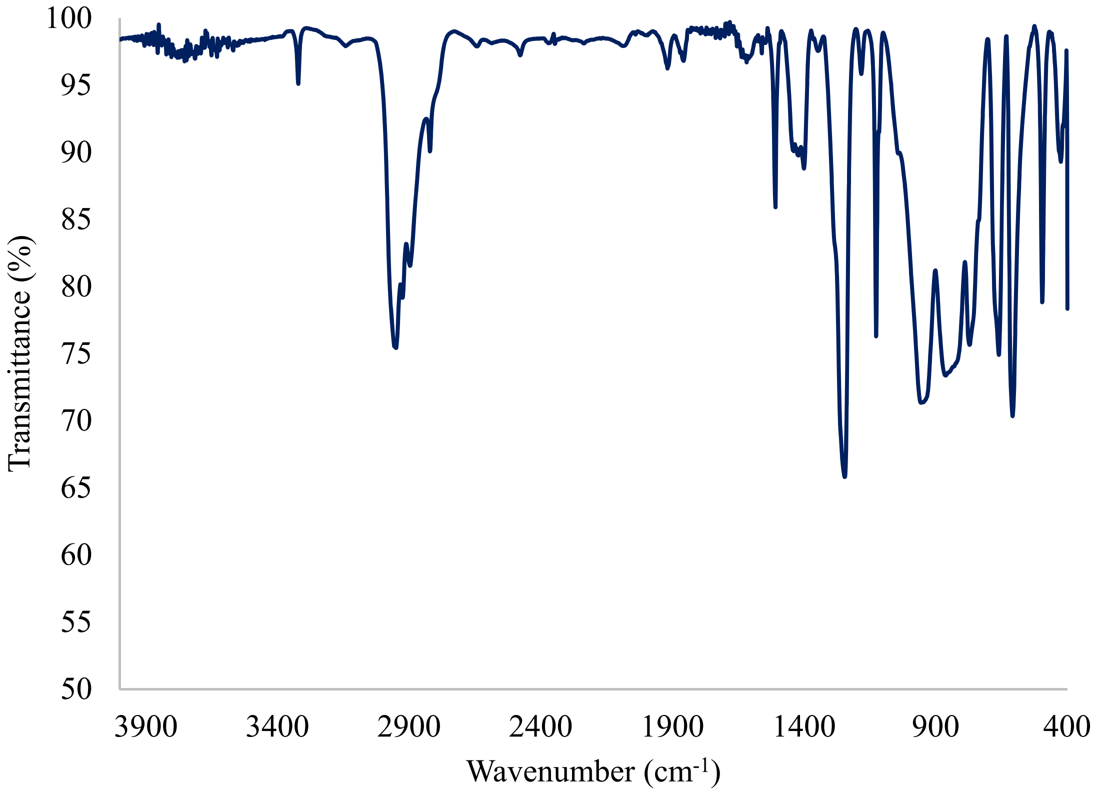

Figure S21. IR spectrum of **2** (KBr pellet).

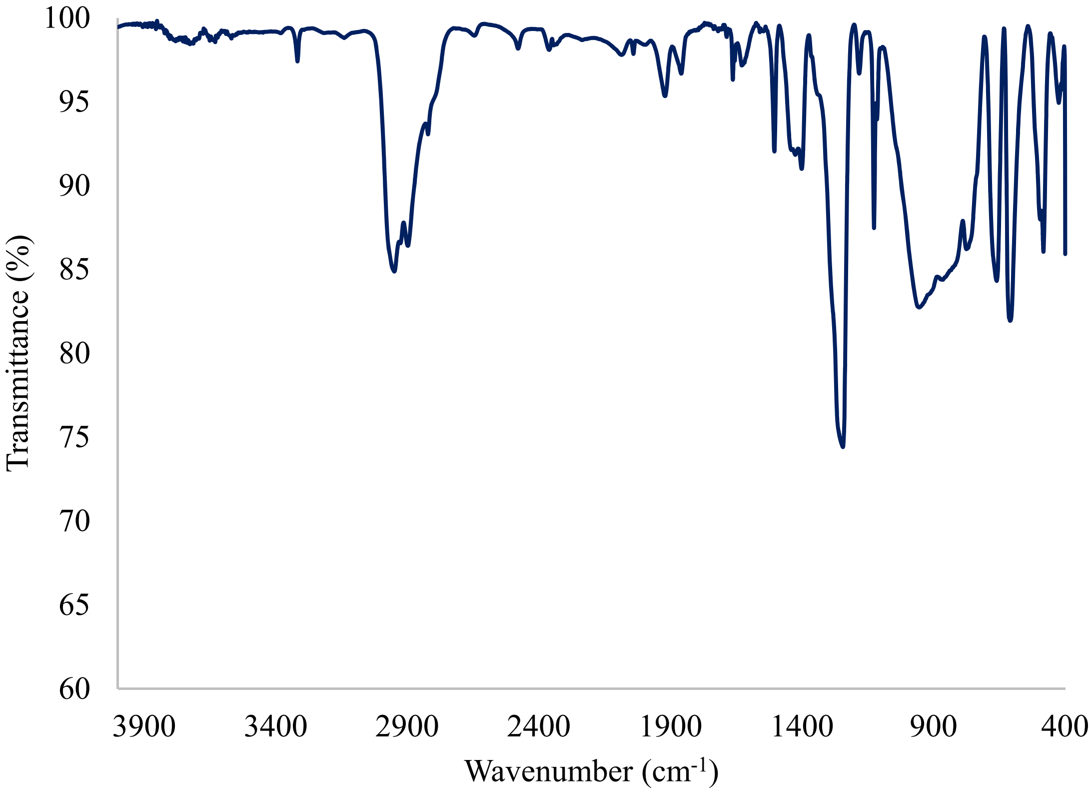

Figure S22. IR spectrum of **2-^{15}N** (KBr pellet).

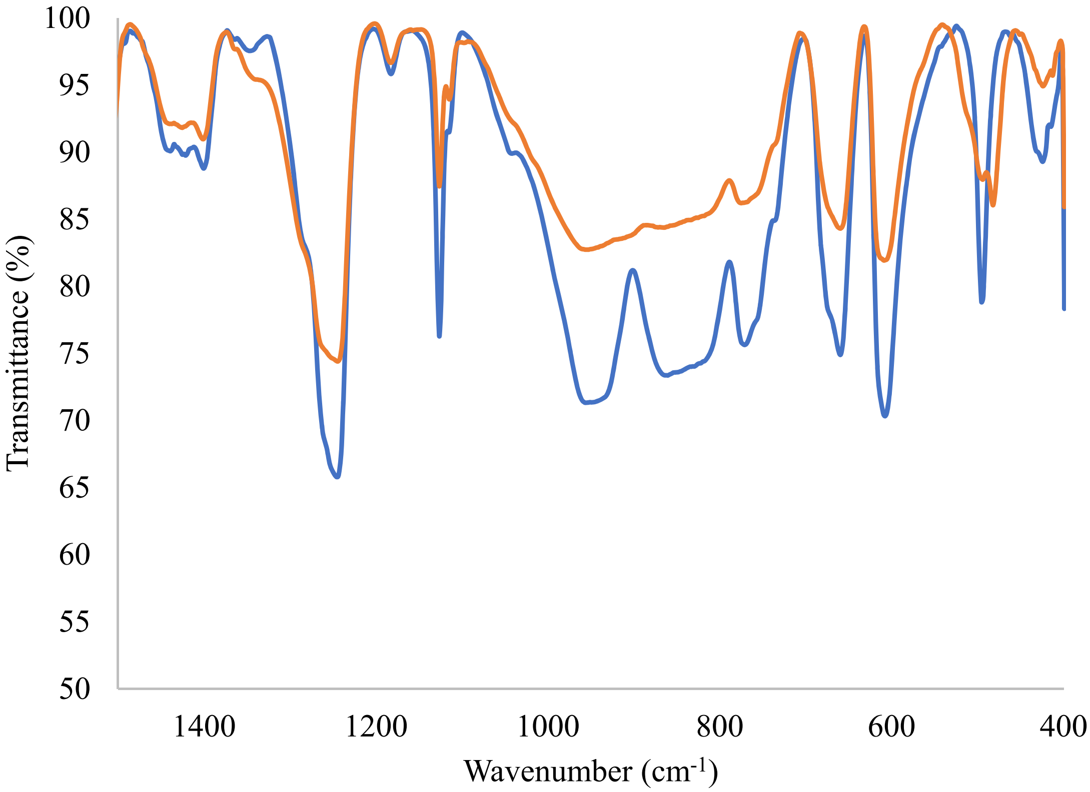

Figure S23. Partial IR spectra of **2-^{15}N** (orange) and **2** (blue) (KBr pellet).

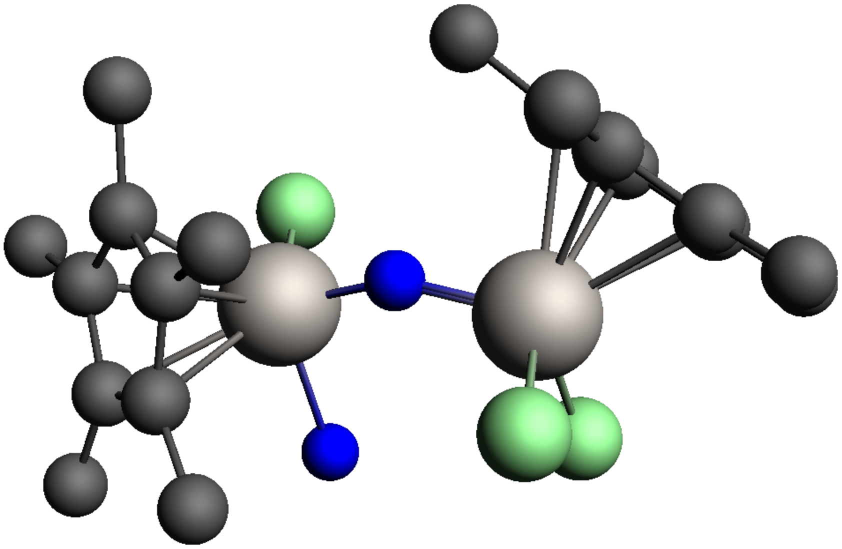

Figure S24. Optimized structure of [{Cp*TiCl$_2$}(μ-N){Cp*TiCl(NH$_3$)}] at the DFT/B3LYP/TZ2P level of theory (using ADF). Hydrogen atoms omitted for clarity. Color code: Ti light gray, N blue, Cl green, C dark gray. Cartesian coordinates are printed below.

Ti	-0.73149487	-0.76769287	1.45060032
Ti	1.09376293	1.14321788	-0.74062345
C	0.36391051	0.53287718	-3.96788162
Cl	-0.00729108	0.60274460	3.19290028
Cl	-0.01433096	3.11473285	-1.09450434
N	0.00000000	0.00000000	0.00000000
N	2.12891761	1.77680256	1.06844488
H	1.47565952	1.60075703	1.84295445
H	2.97718848	1.26129417	1.27603474
H	2.35685541	2.76565719	1.05574511
C	-2.71880292	-2.01671347	1.99735998
C	-2.58192621	-1.96540850	0.58001517
C	-2.72044944	-0.61310980	0.17118451
C	-2.89405901	0.17749554	1.33701156
C	-2.91493829	-0.69504050	2.46409649
H	-0.47135616	-0.10026750	-3.67353501
H	0.70802140	0.19219971	-4.94805953
H	-0.01382530	1.54772939	-4.08249809
C	2.50433304	2.81009715	-3.45263126
H	1.51224854	3.20063312	-3.67228753
H	3.03842213	2.69619191	-4.39990202
H	3.02828228	3.56459629	-2.86753098
C	4.48823386	1.80677120	-1.18988020
C	-2.73624984	-0.10761609	-1.23262717
H	-2.30432352	0.88880351	-1.29937972
H	4.28676827	2.87541224	-1.10706231

H	-2.16602567	-0.75855912	-1.89240492
C	-3.05956332	1.66379884	1.36304862
H	-2.47209407	2.14124512	0.57995742
H	-2.73865446	2.07936080	2.31631869
H	-4.10663436	1.94086077	1.21254062
C	-3.16917421	-0.29379814	3.88063009
H	-4.23824515	-0.34845130	4.10368375
H	-2.83746911	0.72395811	4.07221897
H	-2.65039658	-0.94512197	4.58223537
C	2.90647575	-0.26489057	-1.33656969
C	1.79406969	-0.63225507	-2.13233734
C	1.47398626	0.47454577	-2.96562843
C	2.43016136	1.50488664	-2.72925655
C	3.30754278	1.05325082	-1.71725310
C	3.55609305	-1.14348640	-0.31270883
H	4.20712859	-1.88039467	-0.79018961
H	2.81641500	-1.68757352	0.27418713
H	4.18114442	-0.57457959	0.37681385
C	1.11265873	-1.96028149	-2.10996684
H	5.34830131	1.69408097	-1.85483041
H	4.80194251	1.44420186	-0.21109331
H	0.09563111	-1.88753295	-2.48981648
Cl	0.51775607	-2.66894561	1.75285794
H	1.05840411	-2.36202832	-1.10043563
H	1.65189113	-2.67632271	-2.73608434
H	-3.76149525	-0.06088352	-1.60974901
C	-2.71061518	-3.25633082	2.83120728
H	-3.71300369	-3.69066770	2.88234090
H	-2.38721302	-3.05044485	3.85034810
H	-2.03936771	-4.00703275	2.41900065
C	-2.39493960	-3.14423526	-0.32033482
H	-1.89630473	-2.86153349	-1.24571874
H	-3.35991263	-3.58568136	-0.58424354
H	-1.79252025	-3.91464355	0.15723615

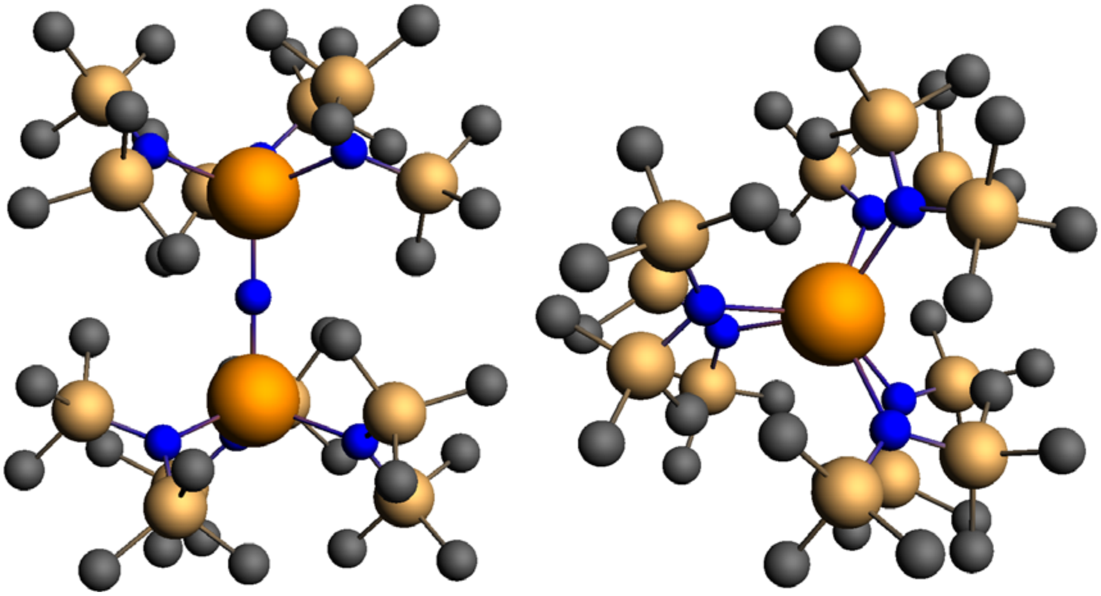

Figure S25. Views along the Y-axis (left) and along the Z-axis (right) of the optimized geometry of $[(R_2N)_3Th(\mu\text{-}N)Th(NR_2)_3]^-$ (R = $SiMe_3$) at the DFT/B3LYP/TZ2P level of theory (using ADF). Hydrogen atoms omitted for clarity. Color code: Th orange, N blue, Si beige, C gray. Cartesian coordinates are printed below.

C	-3.39744725	2.90662531	3.24687966
H	-4.29280930	2.68375624	2.66416894
H	-2.66330788	3.33341724	2.56512363
H	-3.65437673	3.67073877	3.98464860
C	2.48061434	4.38855580	1.71797027
H	3.05707116	3.80740233	1.00135507
H	3.12440676	4.60259331	2.57219026
H	2.22451257	5.34096852	1.25079913
C	0.06687792	4.63229118	3.49101510
H	-0.88874738	4.23388133	3.82735238
H	-0.12853462	5.58751370	2.99584088
H	0.67492363	4.83260100	4.37190190
C	-0.26767066	3.31938151	0.82632502
H	0.15515836	2.80861711	-0.03412515
H	-0.59276996	4.31203600	0.50684929
H	-1.17432199	2.77780156	1.10268500
C	2.70837477	3.19646516	5.25704869
H	2.96946862	4.13007263	4.76002613
H	3.50300966	2.96850567	5.97243476
H	1.78940854	3.35827116	5.82203123
C	4.20803994	1.49980070	3.25344874
H	4.21493168	0.64615817	2.57717172
H	4.99545348	1.34620702	3.99550142
H	4.46332597	2.38340381	2.66623998
C	2.18505812	0.27620273	5.21881162

H	1.98825433	-0.65479009	4.69324421
H	1.32404689	0.49931026	5.85035633
H	3.04481787	0.11133943	5.87241679
C	3.00854583	-1.43229765	0.83283145
H	2.35254544	-1.54036790	-0.02630812
H	4.02906562	-1.65239850	0.51161108
H	2.99868642	-0.37622285	1.10913084
C	3.97341817	-2.37465494	3.50100172
H	4.10652985	-1.34712157	3.83526019
H	4.89900131	-2.68502324	3.00816020
H	3.84062100	-2.99931931	4.38299499
C	2.55451436	-4.34476199	1.72871415
H	3.50645607	-4.60103547	1.26065669
H	1.76181028	-4.55323835	1.01332578
H	2.41808390	-5.00790866	2.58408284
C	-0.81372974	-4.38567691	3.26063239
H	-1.34373667	-4.98804062	4.00259564
H	-0.17612034	-5.05142992	2.67662389
H	-1.55357806	-3.96485583	2.58134279
C	-2.89905428	1.64193606	-0.82793081
H	-2.61141124	1.04417211	0.03225450
H	-3.66425305	2.35270387	-0.50810065
H	-2.02803389	2.23858145	-1.10550554
C	2.20067440	-0.08480501	-5.21960152
H	1.92013380	0.82452521	-4.69394289
H	1.36429739	-0.38319719	-5.85330131
H	3.04366277	0.15696528	-5.87107437
C	4.32200788	-1.13223758	-3.25339153
H	4.25593650	-0.28246533	-2.57546369
H	5.09436512	-0.91123210	-3.99422082
H	4.65064492	-1.99213466	-2.66734195
C	2.97453175	-2.94871502	-5.25942085
H	2.07293908	-3.18864267	-5.82479215
H	3.31474857	-3.85680364	-4.76289045
H	3.74680108	-2.65302777	-5.97447179
C	0.01610005	-3.32937933	-0.83135918
H	0.39324731	-2.78439316	0.02936568
H	-0.22214942	-4.34653532	-0.51245016
H	-0.93386569	-2.86802007	-1.10791093
C	2.84484488	-4.16219162	-1.72116964
H	3.37049280	-3.53545626	-1.00390954
H	3.50482767	-4.32225105	-2.57487032
H	2.66781157	-5.13257432	-1.25421965
C	-1.03828953	1.94908999	-5.21796480
H	-0.36140019	1.37287451	-5.85037614
H	-1.66832294	2.55766963	-5.87074480

H	-1.68596778	1.25251896	-4.69166044
C	-1.19262619	4.30721580	-3.24784803
H	-1.89176217	3.82343732	-2.56728363
H	-1.77430102	4.86400224	-3.98669581
H	-0.61188266	5.02339953	-2.66419705
C	1.05033396	4.05530414	-5.25911758
H	1.66985463	4.80142531	-4.76289169
H	0.40547139	4.57958794	-5.96936565
H	1.70539494	3.39576711	-5.83005741
C	2.87173034	1.68237804	-0.83693650
H	2.21238721	1.73521284	0.02478509
H	3.87181208	1.98586740	-0.51939880
H	2.94853224	0.62912790	-1.11379654
C	3.74851702	2.70539997	-3.50510713
H	3.97050306	1.69228651	-3.83603151
H	4.64430367	3.09747635	-3.01555670
H	3.55963899	3.31258780	-4.38909190
C	2.17366179	4.54789707	-1.72804061
H	1.97950766	5.19802486	-2.58217184
H	3.10252503	4.88226420	-1.26286140
H	1.36876695	4.68877643	-1.00990935
N	0.00000000	0.00000000	0.00000000
N	-2.28536006	0.16000544	2.90637995
N	1.27360889	1.90575245	2.90125991
N	1.01079346	-2.05315943	2.90602888
N	1.43336039	-1.78759380	-2.90336918
N	0.82409715	2.13643910	-2.90520269
Si	0.92663366	3.47426547	2.27016252
Si	2.52713506	1.73158670	4.07449207
Si	2.54242876	-2.54083367	2.27803946
Si	0.23025701	-3.04721698	4.08067495
Si	2.66758959	-1.50573618	-4.07600556
Si	1.22026000	-3.38050765	-2.27453513
Si	-0.04172646	3.06439274	-4.07457613
Si	2.31078718	2.74993902	-2.27957337
Th	-0.00012511	0.00093583	2.10931023
Th	0.00000000	-0.00000000	-2.10936850
C	-4.22541904	1.89317323	-3.49304779
H	-4.65808687	1.42844703	-4.37762783
H	-5.01257763	2.47051354	-3.00013286
H	-3.46044148	2.59386136	-3.82310546
C	1.40471640	-3.93945569	5.26465261
H	0.80757783	-4.51199420	5.97937331
H	2.08147907	-4.63432904	4.76868667
H	2.00559411	-3.22608642	5.83042380
C	-1.32829846	1.76889374	5.21955146

H	-1.09484697	0.91292459	5.85429780
H	-0.42206137	2.05836080	4.69360009
H	-1.61270937	2.59929688	5.87001371
C	-0.85513066	-2.01774146	5.22382380
H	-0.22879400	-1.38556260	5.85469121
H	-1.56030935	-1.37920049	4.69771000
H	-1.43082175	-2.67664041	5.87798998
Si	-3.47123895	-0.92673920	2.28167758
C	-2.74174249	-1.88827929	0.83979759
H	-2.51098669	-1.26922098	-0.02250392
H	-1.81978599	-2.40344604	1.11639387
H	-3.44002824	-2.66620262	0.52311826
C	-5.04216434	-0.04287645	1.72770236
H	-4.82925550	0.74427103	1.00761698
H	-5.73748013	-0.74460127	1.26388149
H	-5.54990960	0.40994573	2.58035396
C	-4.04090407	-2.24694857	3.50790091
H	-4.51776343	-1.81818158	4.38798119
H	-4.77016781	-2.89661106	3.01598239
H	-3.21655178	-2.87293559	3.84513003
Si	-3.54097615	0.62355572	-2.27200505
C	-5.02658959	-0.39971807	-1.72249405
H	-5.78257737	0.23456994	-1.25651555
H	-5.49085107	-0.89278508	-2.57760684
H	-4.74419386	-1.16765558	-1.00549452
Si	-2.75971818	1.33779802	4.07518258
C	-4.12125384	0.77036683	5.25914873
H	-5.06028103	0.52867549	4.76255703
H	-3.80404376	-0.10398515	5.82918616
H	-4.32066140	1.57658665	5.97010554
C	0.46305608	-4.60582733	-3.49782881
H	1.08817591	-4.75448800	-4.37698917
H	0.34666587	-5.57414151	-3.00319872
H	-0.52156249	-4.28848214	-3.83678271
N	-2.26431577	-0.35206539	-2.90227137
C	-3.13688380	-3.18278813	-3.25704574
H	-2.36864660	-3.54952049	-2.57791600
H	-4.04767317	-3.04068001	-2.67310120
H	-3.32798964	-3.96158216	-3.99947807
C	-4.03834218	-1.10680555	-5.26060918
H	-3.79633419	-0.20576536	-5.82592349
H	-4.16656783	-1.92371562	-5.97575736
H	-4.99545639	-0.94895055	-4.76485845
C	-1.17075258	-1.86451119	-5.22079919
H	-1.38464937	-2.71191344	-5.87632761
H	-1.00851511	-0.98857583	-5.85047936

H	-0.24410025	-2.08077241	-4.69529426
Si	-2.63494857	-1.56111600	-4.07676141

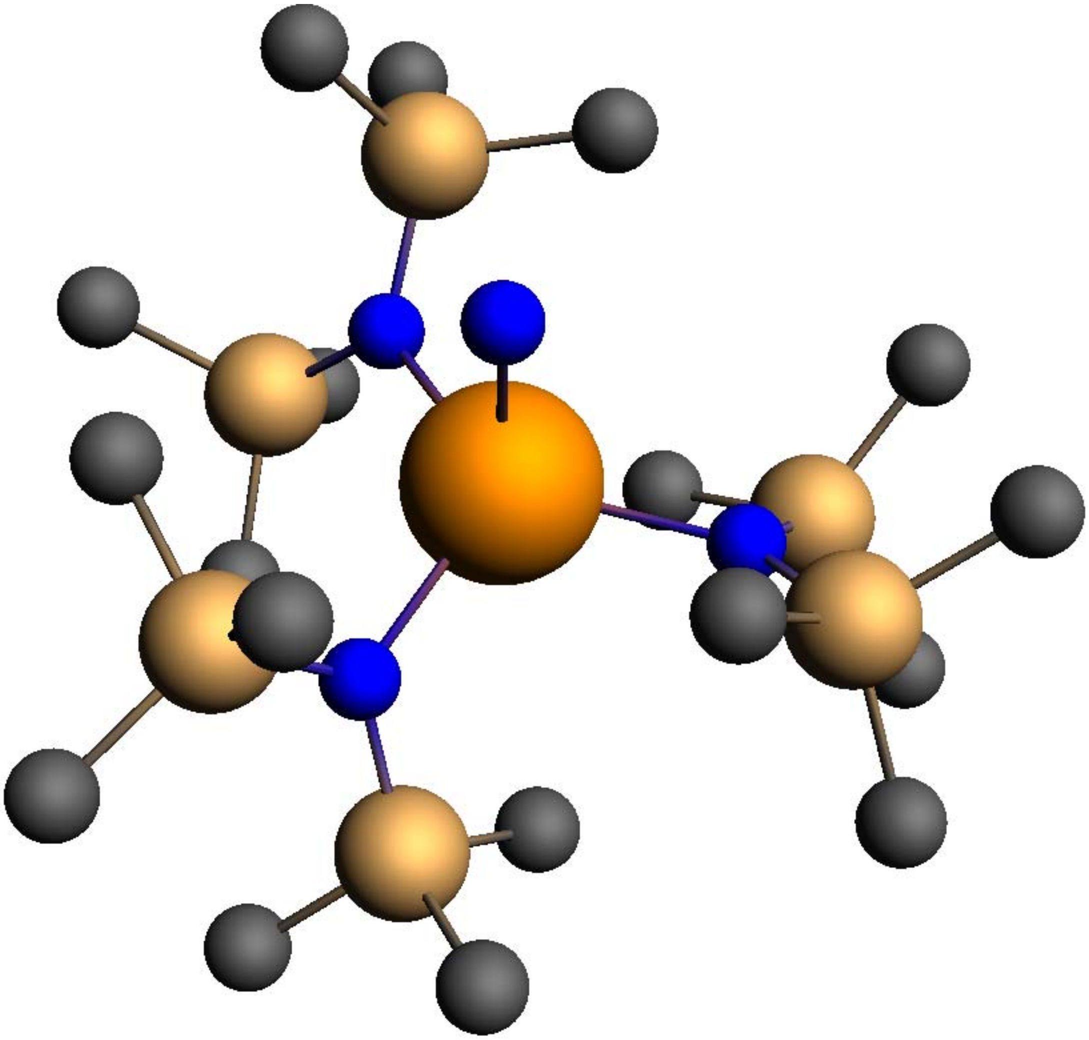

Figure S26. Optimized geometry of [Th(NR$_2$)$_3$(NH$_2$)] (R = SiMe$_3$) at the DFT/B3LYP/TZ2P level of theory (using ADF). Hydrogen atoms omitted for clarity. Color code: Th orange, N blue, Si beige, C gray. Cartesian coordinates are printed below.

Si	-3.40923682	0.03406635	0.86176104
Si	1.70427757	-2.96230216	0.76361240
C	2.50736186	-4.52256301	0.08477690
N	0.84457288	2.13446981	-0.46502442
C	-0.98404181	4.50857923	-0.65391188
Th	0.00000000	0.00000000	0.00000000
N	0.00000000	0.00000000	2.25719717
C	-2.86371927	1.76711967	1.35846623
Si	-2.70977737	-1.77725729	-1.44827851
C	-3.56708913	-1.05342789	2.38918005
C	-3.80929108	-1.05148160	-2.79024498
C	-1.16544733	-2.37667679	-2.34843834
C	-3.56754911	-3.26939597	-0.69467257
N	-2.24633979	-0.61866836	-0.24844079

Si	2.61908714	-1.53243089	-1.77175930
C	-1.34737272	2.00335343	-2.37947630
C	2.60531942	-3.02054466	-2.92137236
C	2.00342689	-0.10185179	-2.84565481
C	4.39538203	-1.19166554	-1.26240718
N	1.58615983	-1.67023420	-0.39278386
C	0.94347267	3.89586971	-2.91763900
Si	2.35300542	2.63332949	0.22163594
Si	-0.07640222	3.12550463	-1.54024395
C	2.92944969	1.34168237	1.47190865
C	3.72776197	2.78568315	-1.05409284
C	-5.13784198	0.21777893	0.14436166
C	-0.03410243	-3.46127637	1.29795064
C	2.70556976	-2.44965021	2.26740104
C	2.20737092	4.27473313	1.12237380
H	-3.51720055	2.14962599	2.14585010
H	-1.84462756	1.81647820	1.74696008
H	-2.94554308	2.44730208	0.51006543
H	-5.78801984	0.67076617	0.89648942
H	-5.58019126	-0.73810855	-0.13691058
H	-5.14283872	0.86438665	-0.73359337
H	-2.61322459	-1.21138554	2.89327549
H	-3.94800037	-2.03769581	2.11199033
H	-4.25793140	-0.61906049	3.11483953
H	-0.56527295	-3.94596012	0.47772498
H	-0.64388860	-2.62647717	1.64485856
H	0.02020680	-4.17488293	2.12311032
H	2.80797537	-3.28061861	2.96881358
H	2.23023933	-1.62183414	2.79118738
H	3.70862330	-2.13448059	1.97381778
H	1.96404910	-4.92900833	-0.76789795
H	2.51149837	-5.28127240	0.87089457
H	3.54269553	-4.36140862	-0.21790852
H	1.89494275	0.84910542	-2.32732118
H	1.05440285	-0.34422569	-3.32939674
H	2.72467703	0.06129417	-3.64974103
H	3.07444529	-2.74424945	-3.86879837
H	1.58566826	-3.34145951	-3.13741550
H	3.15023543	-3.87209129	-2.51922700
H	5.04350952	-1.05718600	-2.13092075
H	4.79165216	-2.02613617	-0.68025676
H	4.46799965	-0.29697532	-0.64388632
H	-1.95725774	2.60362590	-3.05814361
H	-2.04398607	1.50502334	-1.70336302
H	-0.86666563	1.23686654	-2.99439475
H	1.63251715	4.65072849	-2.53725489

H	0.28302496	4.38790150	-3.63522989
H	1.52654166	3.14721985	-3.45484070
H	-0.28218887	5.25791409	-0.28610660
H	-1.54259086	4.13410933	0.20304530
H	-1.68481908	5.01051642	-1.32475499
H	4.65995152	3.06402048	-0.55687994
H	3.51272316	3.54539019	-1.80398669
H	3.90132193	1.84456391	-1.57528013
H	3.12768470	4.50108379	1.66511161
H	1.38593251	4.25236948	1.84025408
H	2.02344711	5.09773041	0.42994942
H	2.82691510	0.30560594	1.14183108
H	2.41784416	1.45015968	2.42797496
H	3.99476292	1.49219758	1.65944960
H	-3.35942612	-0.15196919	-3.21334838
H	-4.80054442	-0.78915429	-2.42486230
H	-3.93363999	-1.77441673	-3.59995572
H	-2.94629210	-3.72753004	0.07562480
H	-3.77769079	-4.02400030	-1.45551152
H	-4.51763286	-2.99417393	-0.23426509
H	-0.41467819	-2.82362278	-1.69988087
H	-0.68314153	-1.57841824	-2.91827224
H	-1.46212857	-3.13264697	-3.07922587
H	-0.74394599	-0.34674713	2.85028796
H	0.73501389	0.34586735	2.85995523

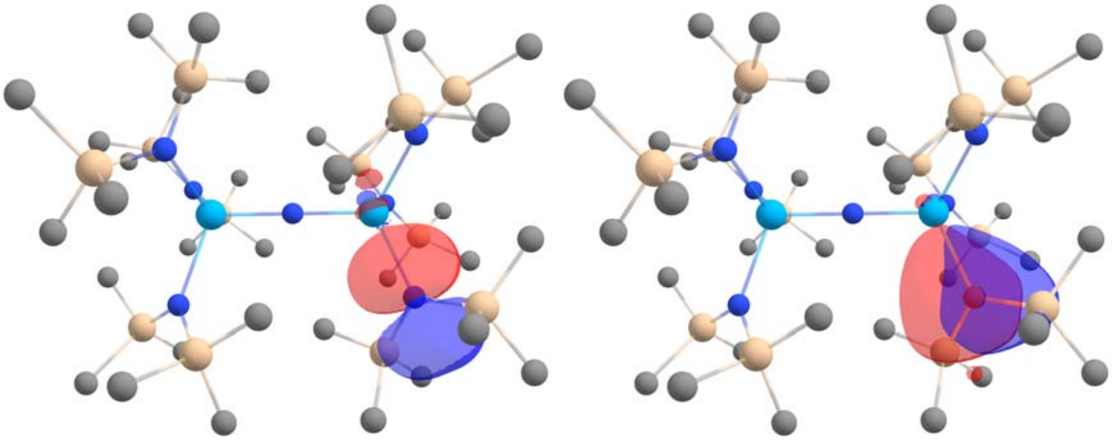

Figure S27. Th−N$_{\text{silylamide}}$ (σ+π) bonding NLMOs in $[(NR_2)_3Th(\mu\text{-}N)Th(NR_2)_3]^-$ (R = SiMe$_3$; isosurface plots ±0.03 au; hydrogen atoms are omitted for clarity). Color code for atoms: Th, light blue; N, blue; Si, beige; C, gray.

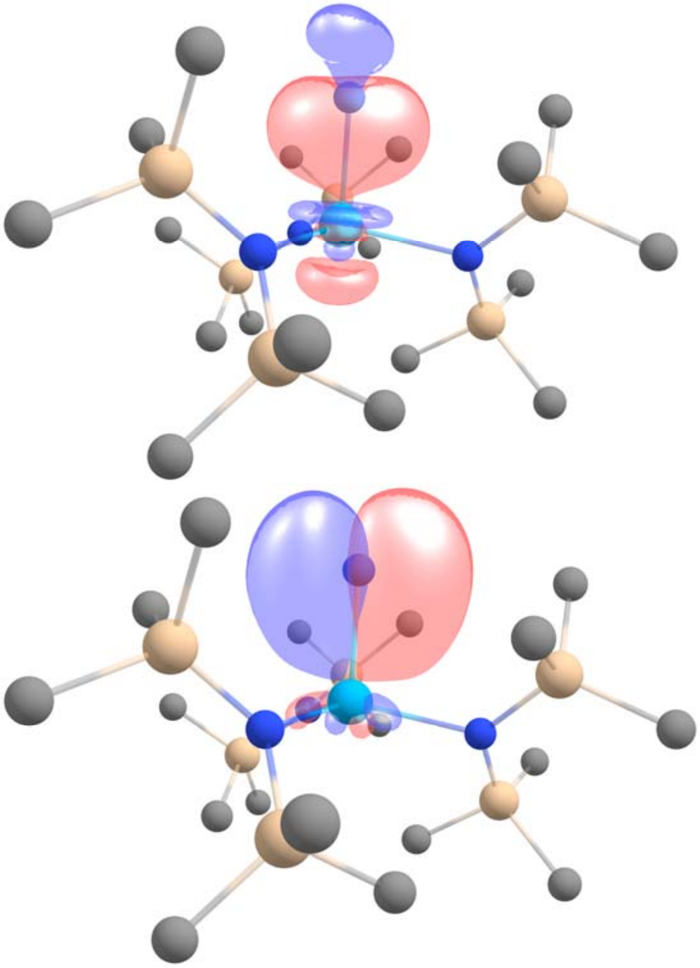

Figure S28. Th−N$_{\mathrm{amide}}$ (σ+π) bonding NLMOs in [Th(NR$_2$)$_3$(NH$_2$)] (R = SiMe$_3$; isosurface plots ±0.03 au; hydrogen atoms are omitted for clarity). Color code for atoms: Th, light blue; N, blue; Si, beige; C, gray.

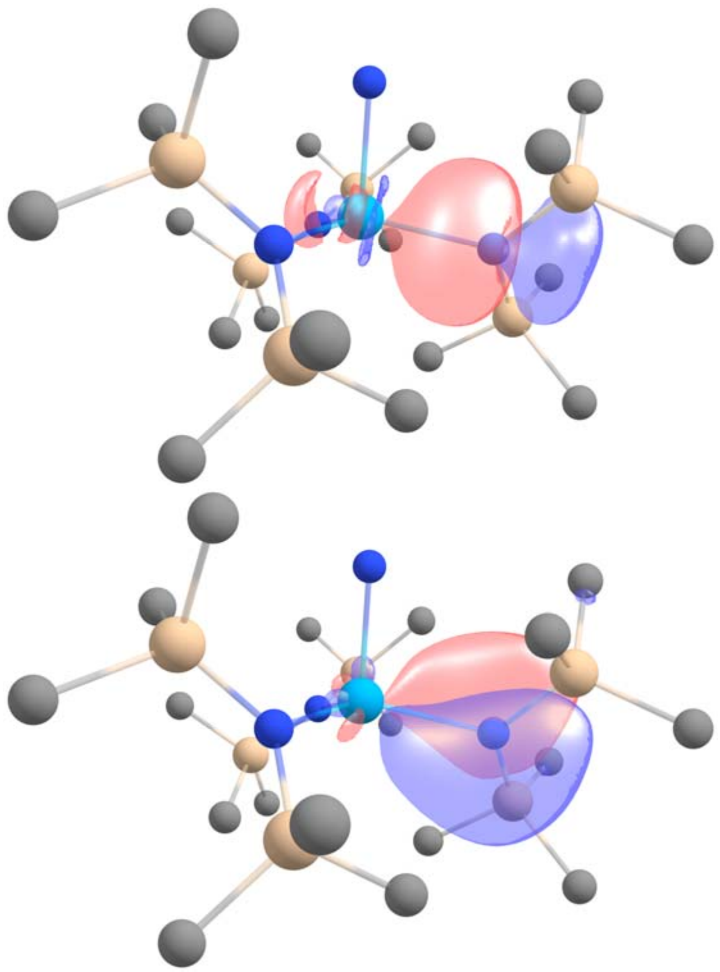

Figure S29. Th−N$_{\text{silylamide}}$ (σ+π) bonding NLMOs in [Th(NR$_2$)$_3$(NH$_2$)] (R = SiMe$_3$; isosurface plots ±0.03 au; hydrogen atoms are omitted for clarity). Color code for atoms: Th, light blue; N, blue; Si, beige; C, gray.

Table S2. % compositions of the Th-N$_{\text{silylamide}}$ Bonding NLMOs in $[(NR_2)_3Th(\mu\text{-}N)Th(NR_2)_3]^-$ and $[Th(NR_2)_3(NH_2)]$ (R = $SiMe_3$).

Complex	**Orbital**	**%N**			**%Th**					**%Si**			
		Total N	2s	2p	Total Th	7s	7p	6d	5f	Total Si	3s	3p	3d
$[Th(NR_2)_3(NH_2)]$	σ	92	31	69	6	8	6	61	25	2	0	94	6
	π	90	0	100	90	0	0	48	52	4	0	89	11
$[(NR_2)_3Th(\mu\text{-}N)Th(NR_2)_3]^-$	σ	94	15	85	4	2	12	62	24	2	7	86	7
	π	90	0	100	4	0	0	52	48	4	0	90	10

Table S3. Calculated Shielding and chemical shifts for DFT/B3LYP/TZ2P optimized geometries of nitromethane, $[\{Cp^*TiCl_2\}(\mu\text{-}N)\{Cp^*TiCl(NH_3)\}]$, $[(NR_2)_3Th(\mu\text{-}N)Th(NR_2)_3]^-$, and $[Th(NR_2)_3(NH_2)]$ (R = $SiMe_3$).

Compound	**Method**	**σ_{calcd} (ppm)**	**δ_{calcd} (ppm)[a]**	**δ_{expt} (ppm)**
$MeNO_2$	PBE0	–159.9	-	-
	SO-PBE0	–156.2	-	-
	B3LYP	–166.7	-	-
	SO-B3LYP	–162.8	-	-
$[\{Cp^*TiCl_2\}(\mu\text{-}N)\{Cp^*TiCl(NH_3)\}]$	PBE0	–566.7	406.8	431.6
	SO-PBE0	–570.7	414.5	
	B3LYP	–588.5	421.8	
	SO-B3LYP	–593.3	430.5	
$[(NR_2)_3Th(\mu\text{-}N)Th(NR_2)_3]^-$	PBE0	–385.9	226.0	298.8
	SO-PBE0	–461.6	305.4	
$[Th(NR_2)_3(NH_2)]$	PBE0	94.0	–253.9	–198.4
	SO-PBE0	53.5	–209.7	

[a] Referenced to nitromethane: $\delta_{calcd} = \sigma_{calcd}$ (N, nitromethane) – σ_{calcd} (N, metal complex). Solvents were used in the calculations (COSMO model): nitromethane for $MeNO_2$, chloroform for $[\{Cp^*TiCl_2\}(\mu\text{-}N)\{Cp^*TiCl(NH_3)\}]$, tetrahydrofuran for $[(NR_2)_3Th(\mu\text{-}N)Th(NR_2)_3]^-$, and benzene for $[Th(NR_2)_3(NH_2)]$.

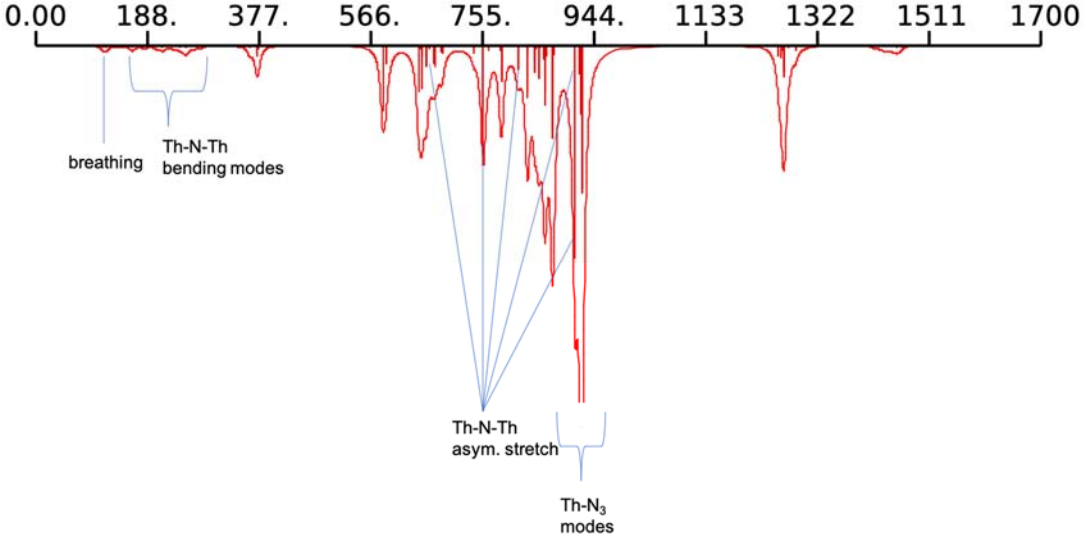

Figure S30. Calculated IR spectrum for **[1]**⁻. The principal Th-N-Th asymmetric stretching mode can be observed at 758.2 cm^{-1}. However, several other modes, at 817, 913.4 and 923 cm^{-1}, also have a Th-N-Th asymmetric stretching component, but they are combined with Th-$N_{silylamide}$ modes. Moreover, modes at 588.1, 648.6, 654, 673 cm^{-1} are a combination of the Th-N-Th asymmetric stretch along with various modes of the whole molecular skeleton. There is a breathing mode at 113 cm^{-1} which is not very intense. Finally, there are Th-N-Th bending modes at 254.1, 255.2, 268 and 281.6 cm^{-1}.

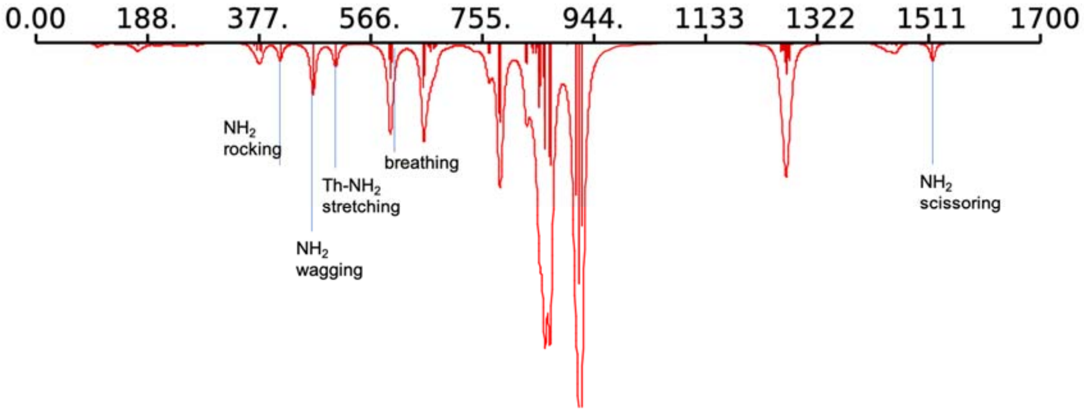

Figure S31. Calculated IR spectrum for **2**. Assignments (cm^{-1}): 414.7 (NH_2 rocking), 470.1 (NH_2 wagging), 508.4 (Th-NH_2 stretching), 613.5 (Th-N breathing), 1518.8 (NH_2 scissoring).

References

1. Cantat, T.; Scott, B. L.; Kiplinger, J. L., Convenient access to the anhydrous thorium tetrachloride complexes $ThCl_4(DME)_2$, $ThCl_4(1,4\text{-dioxane})_2$ and $ThCl_4(THF)_{3.5}$ using commercially available and inexpensive starting materials. *Chem. Commun.* **2010,** *46* (6), 919-21.
2. Bell, N. L.; Maron, L.; Arnold, P. L., Thorium Mono- and Bis(imido) Complexes Made by Reprotonation of *cyclo*-Metalated Amides. *J. Am. Chem. Soc.* **2015,** *137* (33), 10492-5.
3. Harris, R. K.; Becker, E. D.; Cabral de Menezes, S. M.; Goodfellow, R.; Granger, P., NMR nomenclature: nuclear spin properties and conventions for chemical shifts. IUPAC Recommendations 2001. International Union of Pure and Applied Chemistry. Physical Chemistry Division. Commission on Molecular Structure and Spectroscopy. *Magn. Reson. Chem.* **2002,** *40* (7), 489-505.
4. Harris, R. K.; Becker, E. D.; De Menezes, S. M. C.; Granger, P.; Hoffman, R. E.; Zilm, K. W., Further Conventions for NMR Shielding and Chemical Shifts (IUPAC Recommendations 2008). *Magn. Reson. Chem.* **2008,** *46* (6), 582-598.
5. SMART Apex II, v., Bruker AXS Inc., Madison, WI, 2004. .
6. SAINT Software User's Guide, v. a., Bruker AXS Inc., Madison, WI, 2005.
7. SADABS, University of Göttingen, Germany, 2005.
8. SHELXTL, version 6.12, Bruker AXS Inc., Madison, WI, 2005.
9. Baerends, E. J.; Ziegler, T.; Atkins, A. J.; Autschbach, J.; Bashford, D.; Baseggio, O.; Brces, A.; Bickelhaupt, F. M.; Bo, C.; Boerritger, P. M.; Cavallo, L.; Daul, C.; Chong, D. P.; Chulhai, D. V.; Deng, L.; Dickson, R. M.; Dieterich, J. M.; Ellis, D. E.; van Faassen, M.; Ghysels, A.; Giammona, A.; van Gisbergen, S. J. A.; Goez, A.; Gtz, A. W.; Gusarov, S.; Harris, F. E.; van den Hoek, P.; Hu, Z.; Jacob, C. R.; Jacobsen, H.; Jensen, L.; Joubert, L.; Kaminski, J. W.; van Kessel, G.; Knig, C.; Kootstra, F.; Kovalenko, A.; Krykunov, M.; van Lenthe, E.; McCormack, D. A.; Michalak, A.; Mitoraj, M.; Morton, S. M.; Neugebauer, J.; Nicu, V. P.; Noodleman, L.; Osinga, V. P.; Patchkovskii, S.; Pavanello, M.; Peeples, C. A.; Philipsen, P. H. T.; Post, D.; Pye, C. C.; Ramanantoanina, H.; Ramos, P.; Ravenek, W.; Rodrguez, J. I.; Ros, P.; Rger, R.; Schipper, P. R. T.; Schlns, D.; van Schoot, H.; Schreckenbach, G.; Seldenthuis, J. S.; Seth, M.; Snijders, J. G.; Solà, M., ADF2017, SCM, Theoretical Chemistry, Vrije Universiteit, Amsterdam, The Netherlands, https://www.scm.com.
10. Becke, A. D., Density-functional exchange-energy approximation with correct asymptotic behavior. *Phys. Rev. A* **1988,** *38* (6), 3098.
11. Lee, C.; Yang, W.; Parr, R. G., Development of the Colle-Salvetti correlation-energy formula into a functional of the electron density. *Phys. Rev. B* **1988,** *37* (2), 785.
12. Stephens, P. J.; Devlin, F. J.; Chabalowski, C. F.; Frisch, M. J., *Ab initio* Calculation of Vibrational Absorption and Circular Dichroism Spectra Using Density Functional Force Fields. *J. Phys. Chem.* **1994,** *98* (45), 11623-11627.
13. Lenthe, E. v.; Baerends, E. J.; Snijders, J. G., Relativistic regular two-component Hamiltonians. *J. Chem. Phys.* **1993,** *99* (6), 4597-4610.
14. Grimme, S.; Antony, J.; Ehrlich, S.; Krieg, H., A consistent and accurate *ab initio* parametrization of density functional dispersion correction (DFT-D) for the 94 elements H-Pu. *J. Chem. Phys.* **2010,** *132* (15), 154104.

15. Grimme, S.; Ehrlich, S.; Goerigk, L., Effect of the damping function in dispersion corrected density functional theory. *J. Comput. Chem.* **2011,** *32* (7), 1456-1465.

16. Adamo, C.; Barone, V., Toward chemical accuracy in the computation of NMR shieldings: the PBE0 model. *Chem. Phys. Lett.* **1998,** *298* (1), 113-119.

17. Perdew, J. P.; Burke, K.; Ernzerhof, M., Generalized Gradient Approximation Made Simple. *Phys. Rev. Lett.* **1996,** *77* (18), 3865.

18. Klamt, A., Conductor-Like Screening Model for Real Solvents - A New Approach to the Quantitative Calculation of Solvation Phenomena. *J. Phys. Chem.* **1995,** *99* (7), 2224-2235.

19. Pye, C. C.; Ziegler, T., An implementation of the conductor-like screening model of solvation within the Amsterdam density functional package. *Theor. Chem. Acc.* **1999,** *101* (6), 396-408.

20. Autschbach, J., The role of the exchange-correlation response kernel and scaling corrections in relativistic density functional nuclear magnetic shielding calculations with the zeroth-order regular approximation. *Mol. Phys.* **2013,** *111* (16-17), 2544-2554.

21. Frisch, M. J.; Trucks, G. W.; Schlegel, H. B.; Scuseria, G. E.; Robb, M. A.; Cheeseman, J. R.; Scalmani, G.; Barone, V.; Petersson, G. A.; Nakatsuji, H.; Li, X.; Caricato, M.; Marenich, A. V.; Bloino, J.; Janesko, B. G.; Gomperts, R.; Mennucci, B.; Hratchian, H. P.; Ortiz, J. V.; Izmaylov, A. F.; Sonnenberg, J. L.; Williams; Ding, F.; Lipparini, F.; Egidi, F.; Goings, J.; Peng, B.; Petrone, A.; Henderson, T.; Ranasinghe, D.; Zakrzewski, V. G.; Gao, J.; Rega, N.; Zheng, G.; Liang, W.; Hada, M.; Ehara, M.; Toyota, K.; Fukuda, R.; Hasegawa, J.; Ishida, M.; Nakajima, T.; Honda, Y.; Kitao, O.; Nakai, H.; Vreven, T.; Throssell, K.; Montgomery Jr., J. A.; Peralta, J. E.; Ogliaro, F.; Bearpark, M. J.; Heyd, J. J.; Brothers, E. N.; Kudin, K. N.; Staroverov, V. N.; Keith, T. A.; Kobayashi, R.; Normand, J.; Raghavachari, K.; Rendell, A. P.; Burant, J. C.; Iyengar, S. S.; Tomasi, J.; Cossi, M.; Millam, J. M.; Klene, M.; Adamo, C.; Cammi, R.; Ochterski, J. W.; Martin, R. L.; Morokuma, K.; Farkas, O.; Foresman, J. B.; Fox, D. J. *Gaussian 16 Rev. B.01*, Wallingford, CT, 2016.

22. Weigend, F.; Ahlrichs, R., Balanced basis sets of split valence, triple zeta valence and quadruple zeta valence quality for H to Rn: Design and assessment of accuracy. *Phys. Chem. Chem. Phys.* **2005,** *7* (18), 3297-3305.

23. Weigand, A.; Cao, X.; Hangele, T.; Dolg, M., Relativistic Small-Core Pseudopotentials for Actinium, Thorium, and Protactinium. *J. Phys. Chem. A* **2014,** *118* (13), 2519-2530.

24. Glendening, E. D.; Landis, C. R.; Weinhold, F., *NBO 6.0*: Natural bond orbital analysis program. *J. Comput. Chem.* **2013,** *34* (16), 1429-1437.